Electronic Supplementary Information

for

Sustainable phosphorescent oscillators based on photochemical deoxygenation in convections

Hongqi Zhou, Sihan Chen, Jiang He and Wei Lu*

Department of Chemistry, Southern University of Science and Technology (SUSTech), Shenzhen, Guangdong 518055, P. R. China

*E-mail: luw@sustech.edu.cn

Materials. All reagents and solvents were used as received unless otherwise indicated. **Solvents**: Spectroscopic grade dimethyl sulfoxide (DMSO), analytical grade tetramethylene sulfoxide (TMSO), 1,3-dimethyl-3,4,5,6-tetrahydro-2(1H)-pyrimidinone (DMPU), 1-butanol, and *N*, *N*-dimethylformamide were purchased from J&K Scientific Ltd. **Solutes**: Pt(II) octaethylporphyrin (Pt(OEP)), Pd(II) tetraphenyltetrabenzoporphyrin (Pd(TPBP)), and Pt(II) meso-tetraphenyl tetrabenzoporphine (Pt(TPBP)) were purchased from Frontier Scientific, Inc. 9,10-Diphenylanthracene (DPA) was purchased from Alfa Aesar. 9,10-Bis(phenylethynyl)anthracene (BPEA) were purchased from Tokyo Chemical Industry (Shanghai). The platinum complex Pt(NI) was synthesized according to the literature.[1] The gold complex Au(OP) and Au(CN) was synthesized according to the literature.[2]

Spectroscopic characterization. UV-Vis absorption spectra were recorded on a Thermo Scientific Evolution 201 UV-Visible Spectrophotometer. Photo-emission and excitation spectra were recorded on Edinburg spectrometer FLS-980 equipped with a Xe light source and an MCPPMT detector in a cooled housing (–20 °C) which covers a range of 200–870 nm. Another spectrofluorometer is Edinburg spectrometer FS5 equipped with a Xe light source. Emission traces were recorded by using the multiple scan mode and the shutter was set as always open. Emission intensity at fixed wavelength versus time elapsed was recorded by using the kinetic scan mode and the shutter was set as always open. All the measurements have been done at room temperature (ca. 25 °C) unless otherwise indicated. Optical power of xenon lamp in the FLS-980/FS5 fluorimeter and optical power density (OPD) of UV flashlight were measured using a ThorLabs (Newton, NJ, USA) Energy Console Meter (PM100D) equipped with a Photodiode Power Sensor, 200–1100 nm (S120VC). Optical power of diode lasers was measured using a CNI Thermoelectric Laser Power Meter (TS50+TP100) which covers a wavelength range of 190 nm–25 μm (Changchun New Industries Optoelectronics Technology Co., Ltd., China).

FFT (fast Fourier transformation) analyses were performed by an ORIGIN software package.

The Stern–Volmer (K_{SV}) and the bimolecular quenching constants (k_q) were estimated according to the dynamic Stern–Volmer relation, $\tau_0/\tau = 1 + K_{SV}[Q]$, where τ_0 and τ are the phosphorescence lifetimes of Pt(OEP) at 645 nm in the absence or presence of the Pt(TPBP) quencher (Q), respectively. K_{SV} is the Stern–Volmer constant, $K_{SV} = k_q\tau_0$, and [Q] is the molar concentration of Pt(TPBP). The decay curves were recorded on Edinburg spectrometer FLS-980.

Viscosity characterization at room temperature. Kinematic viscosity of DMSO/DMPU/TMSO was measured using the Ubbelohde viscometer (model-1834). Density of DMSO/DMPU/TMSO was measured by weighing a certain volume (10 mL) of DMSO/DMPU/TMSO. Dynamic viscosity η was obtained by multiplying kinematic viscosity and density.

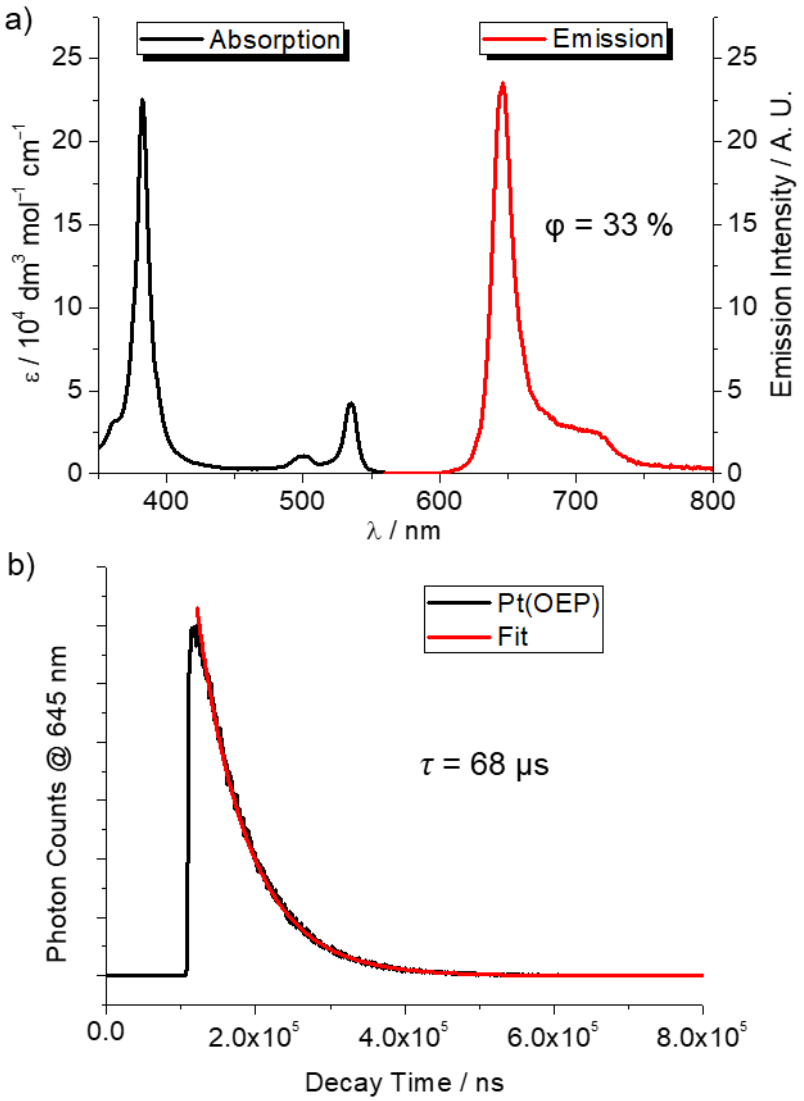

Figure S1. (a) Absorption and emission spectrum of a degassed TMSO solution of Pt(OEP) (5.0×10^{-6} mol dm^{-3}) upon excitation at 532 nm; (b) Lifetime of a degassed TMSO solution of Pt(OEP) (5.0×10^{-6} mol dm^{-3}) upon excitation at 532 nm. The quantum yield and lifetime were 33% and 68 µs, respectively.

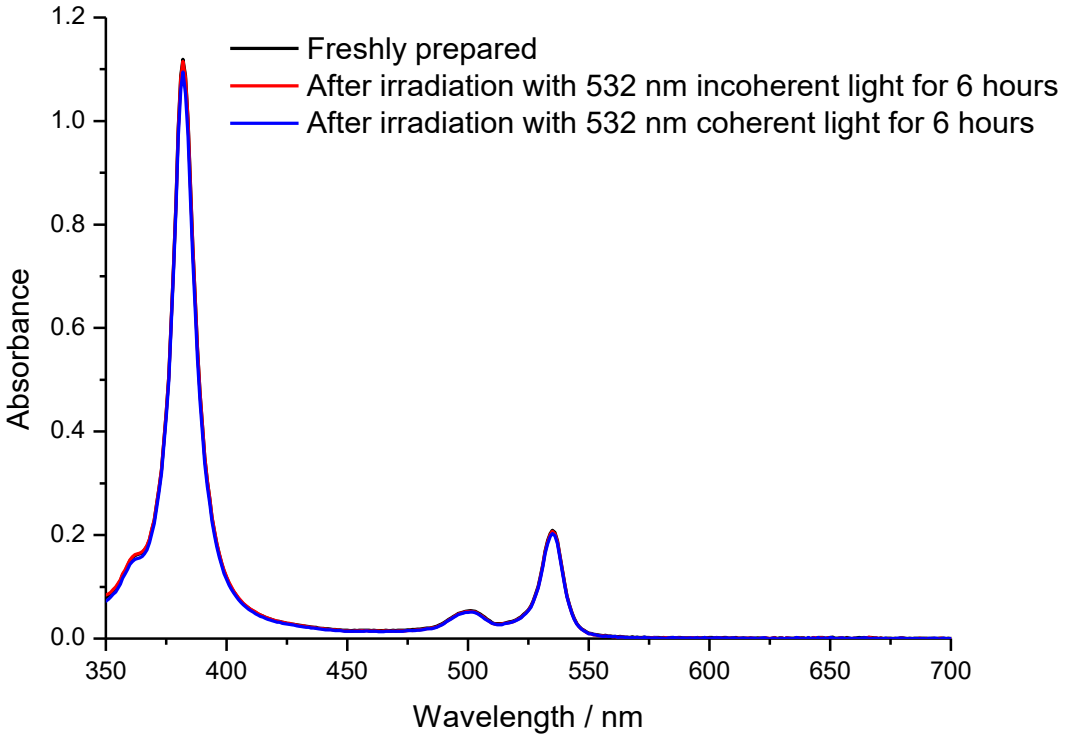

Figure S2. Absorption spectrum of Pt(OEP) (5.0×10^{-6} mol dm^{-3}) in aerated TMSO solution under air: freshly prepared (black line); after 532 nm incoherent irradiation of xenon lamp at 16.0 mW cm^{-2} (red line); after 532 nm coherent irradiation of a continuous-wave laser at 54.5 mW cm^{-2} (bule line).

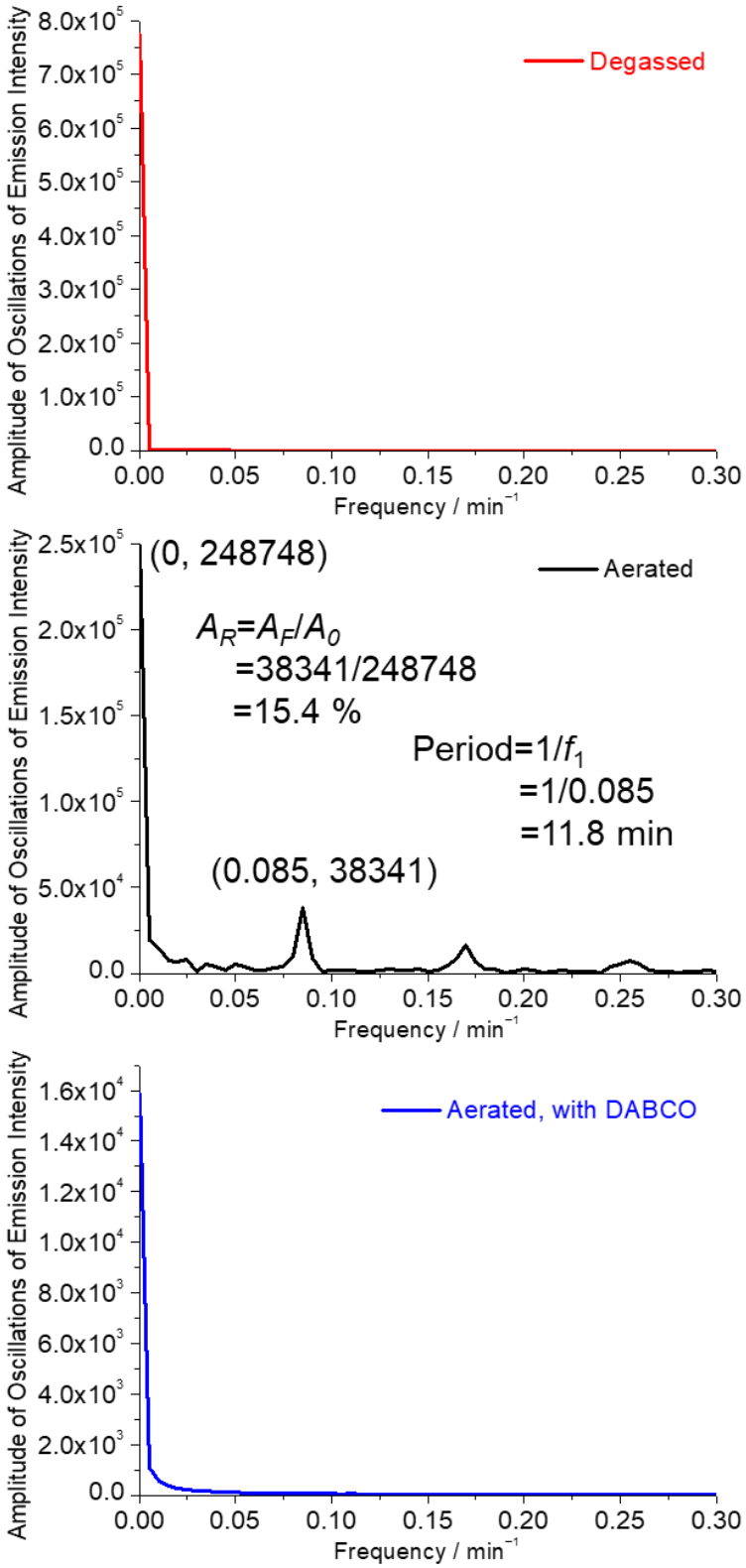

Figure S3. Fourier spectrum (calculated in the time window [100, 300] min) of emission spectrum in Figure 2c. A relative amplitude (A_R) is defined as the amplitude value of fundamental frequency (A_F) divided by the amplitude value of zero frequency (A_0), i.e., $A_R=A_F/A_0$.

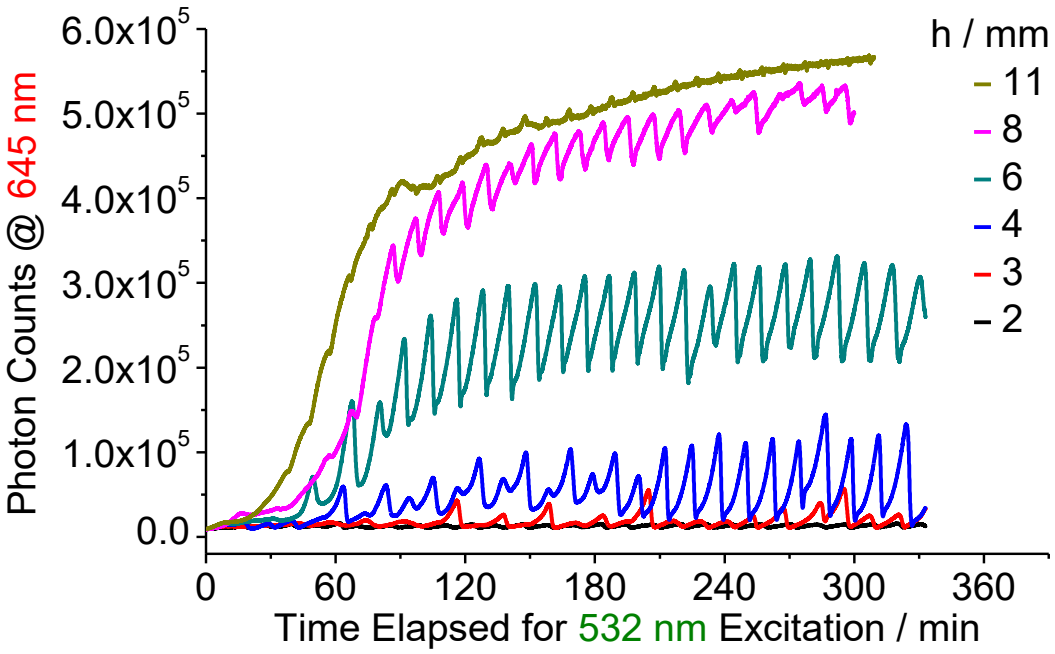

Figure S4. Kinetic emission traces of TMSO solution at different heights when OPD is 1.1 mW cm^{-2} and concentration of Pt(OEP) is 5.0×10^{-6} mol dm^{-3} at 25 °C.

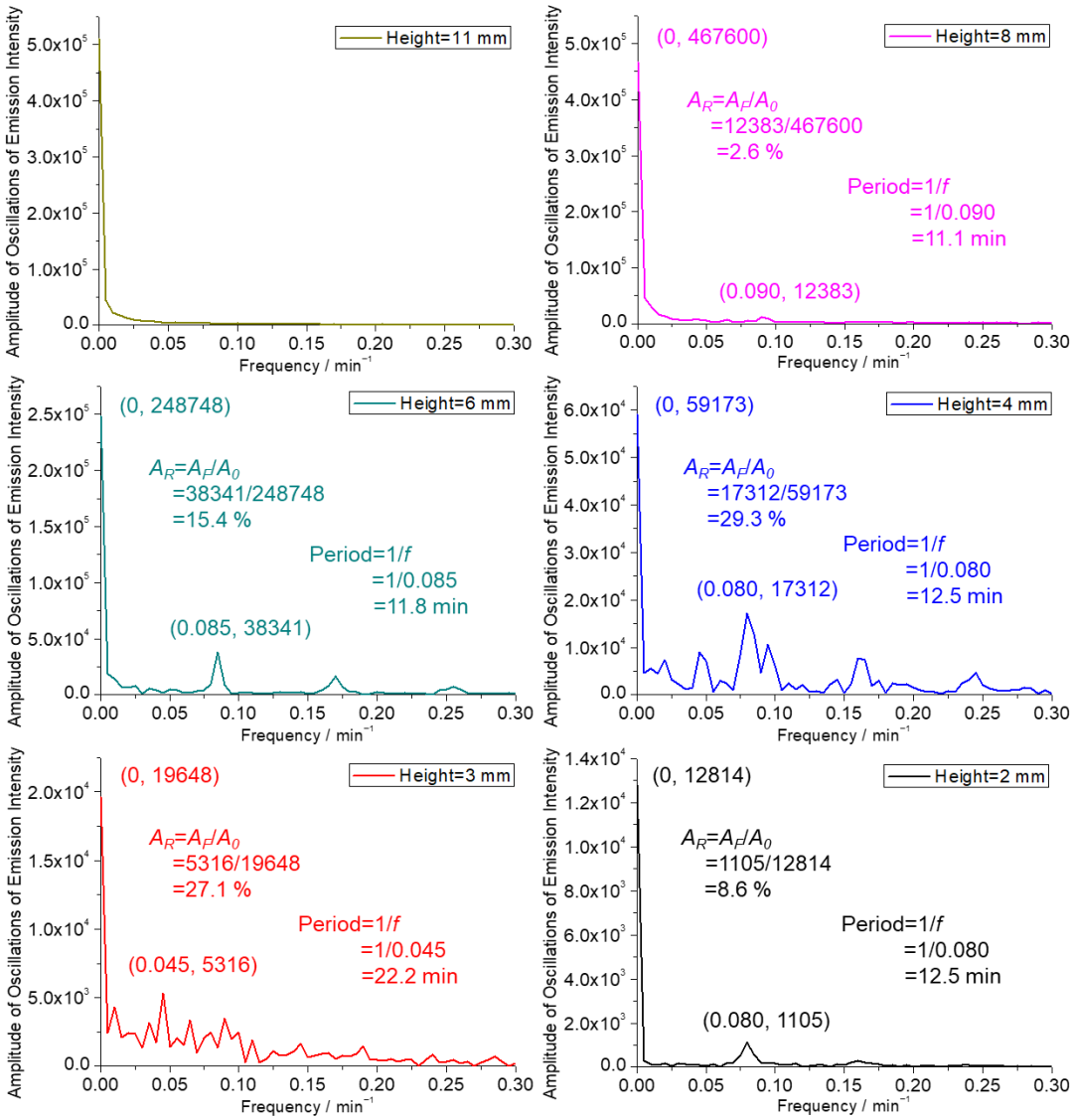

Figure S5. Fourier spectrum (calculated in the time window [100, 300] min) of kinetic emission spectrum of Figure S4.

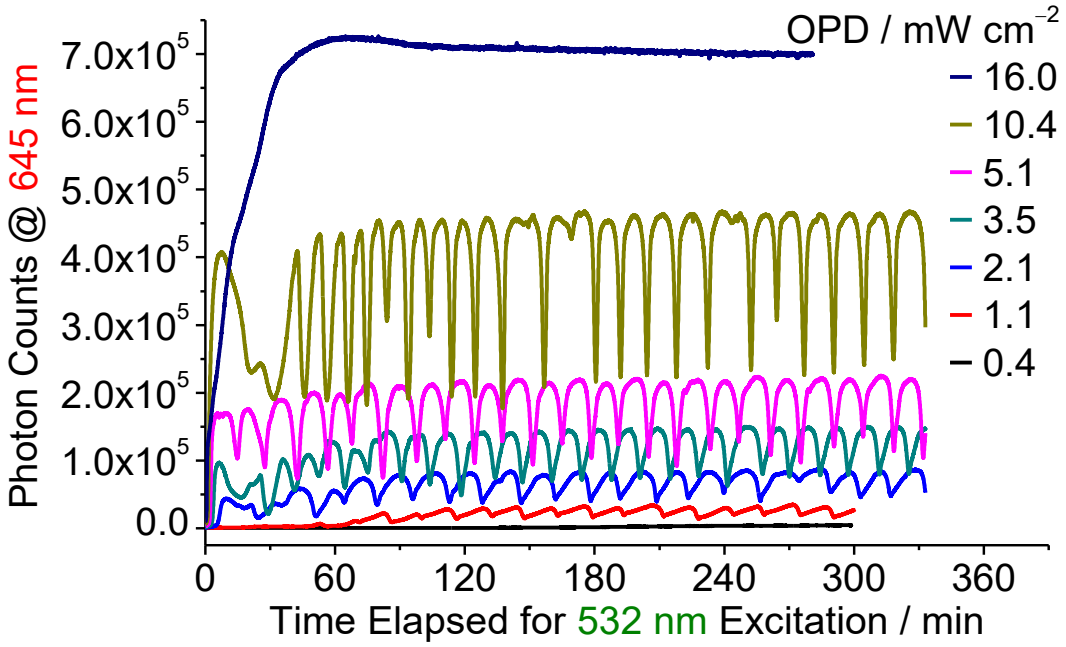

Figure S6. Kinetic emission traces of TMSO solution at different OPD when height is 6 mm and concentration of Pt(OEP) is 5.0×10^{-6} mol dm^{-3} at 25 °C.

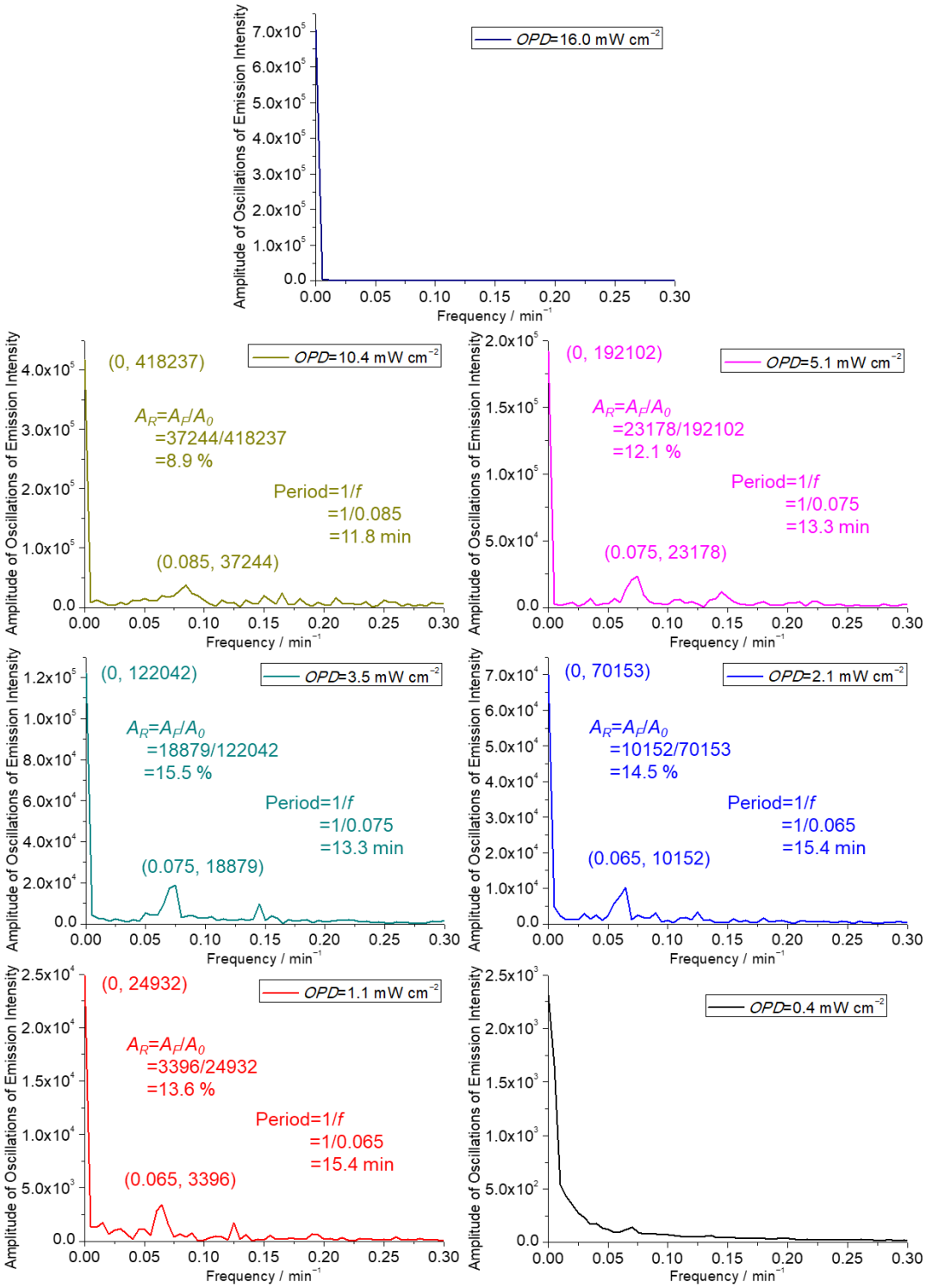

Figure S7. Fourier spectrum (calculated in the time window [100, 300] min) of kinetic emission spectrum of Figure S6.

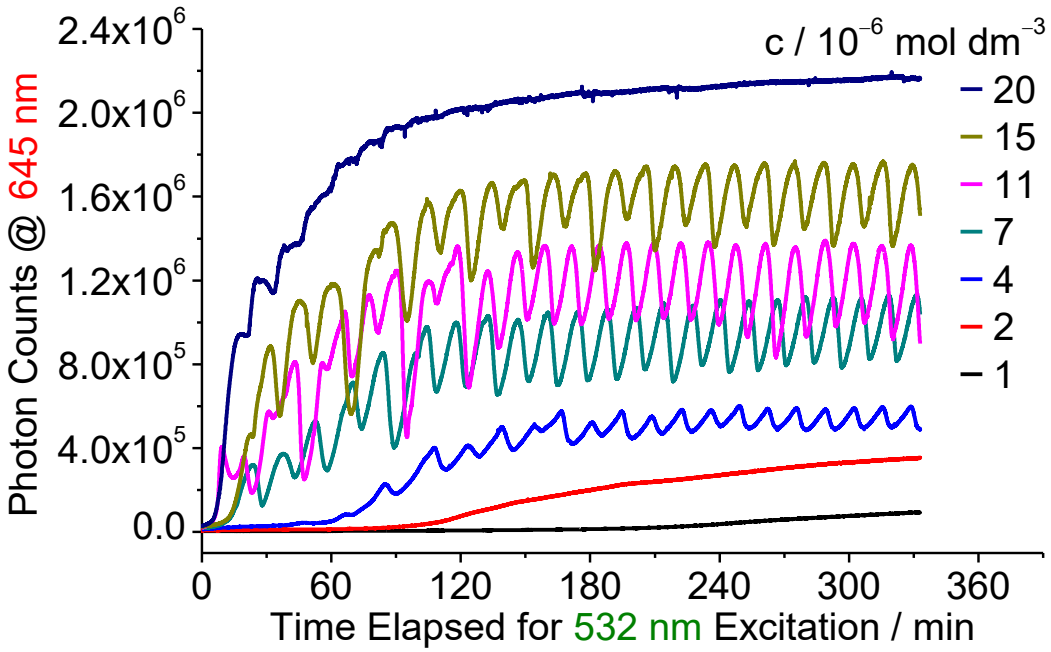

Figure S8. Kinetic emission traces of TMSO solution at different concentrations of Pt(OEP) when the height is 6 mm and OPD is 1.1 mW cm^{-2} at 25 °C.

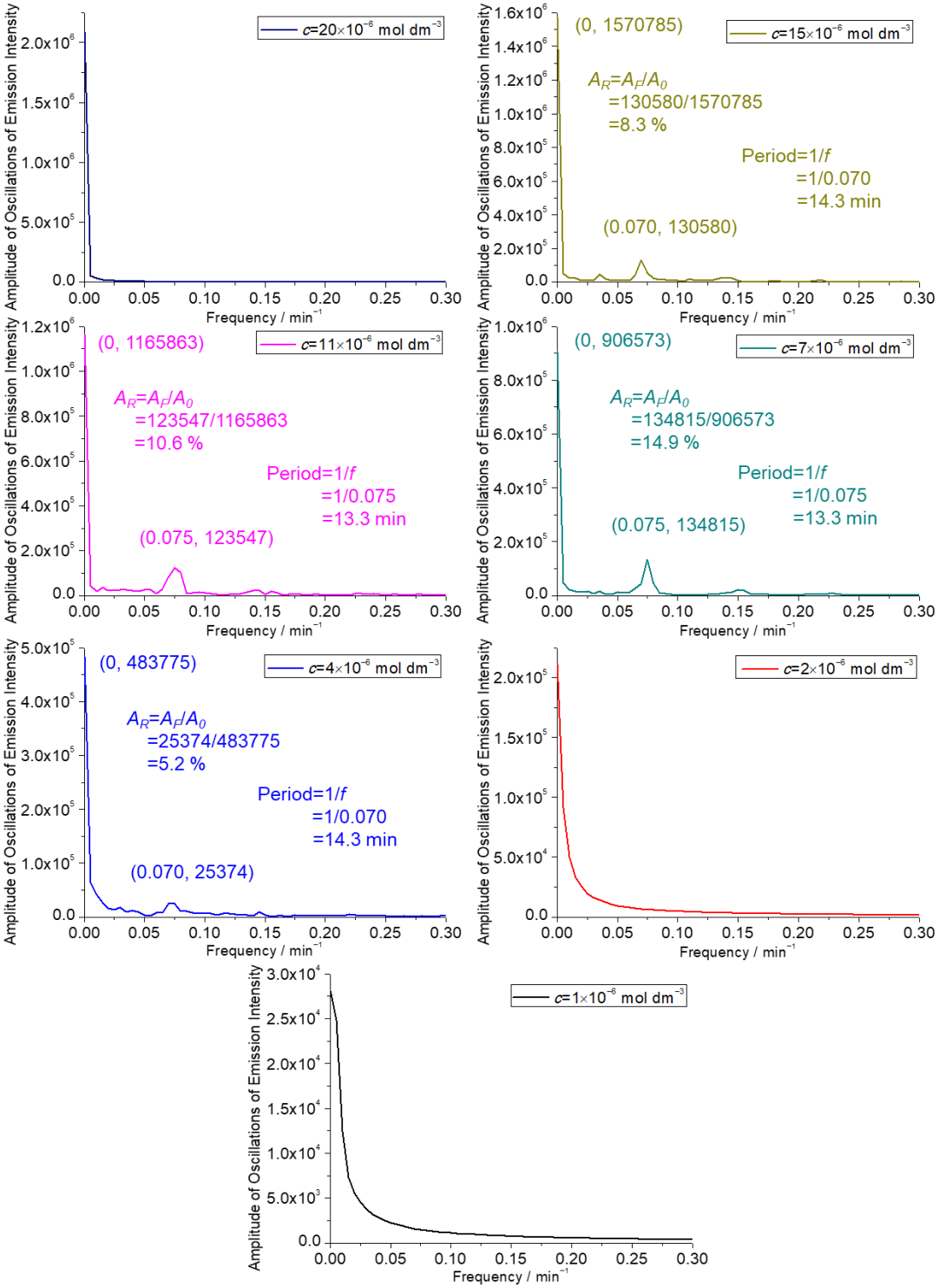

Figure S9. Fourier spectrum (calculated in the time window [100, 300] min) of kinetic emission spectrum of Figure S8.

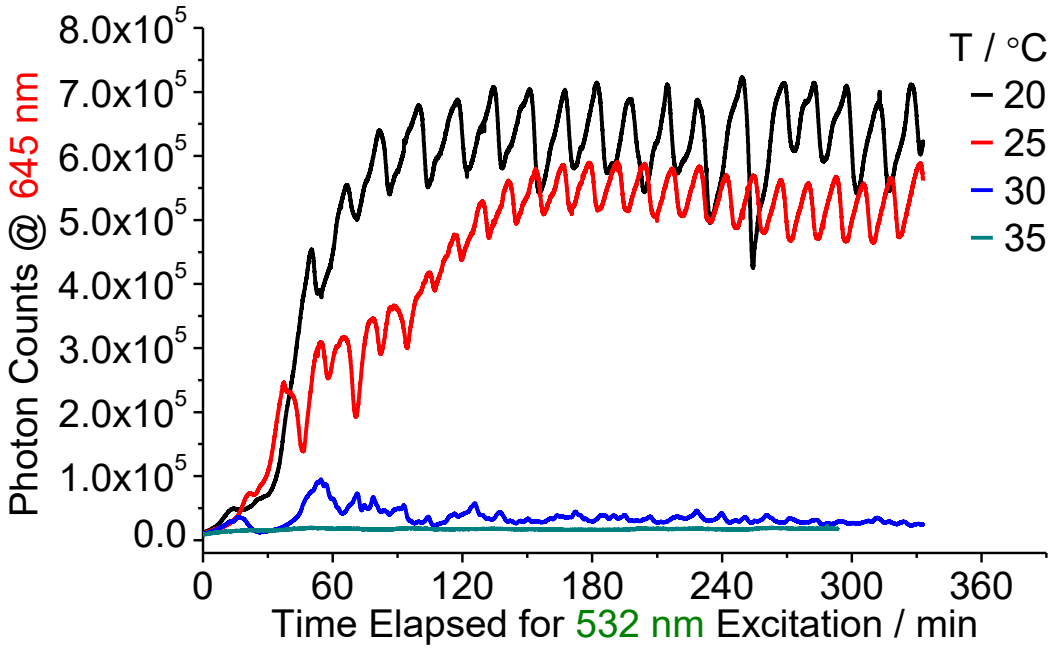

Figure S10. Kinetic emission traces of TMSO solution at different temperatures when the height is 6 mm, OPD is 1.1 mW cm^{-2} and concentration of Pt(OEP) is 5.0×10^{-6} mol dm^{-3}.

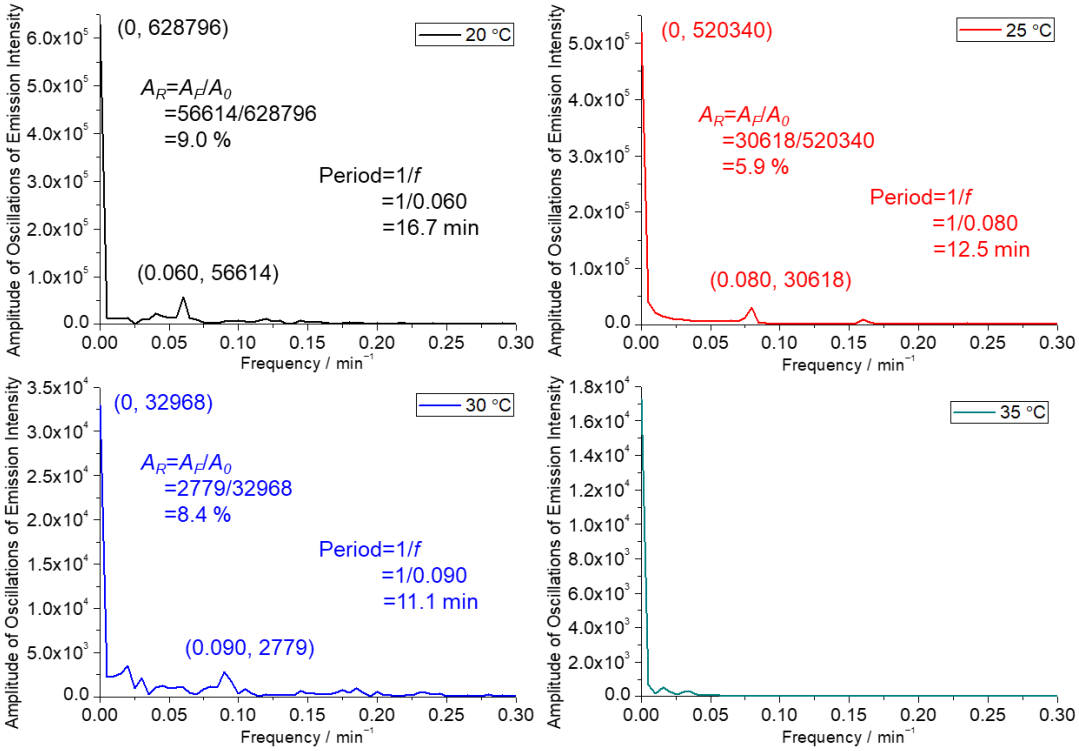

Figure S11. Fourier spectrum (calculated in the time window [100, 300] min) of kinetic emission spectrum of Figure S10.

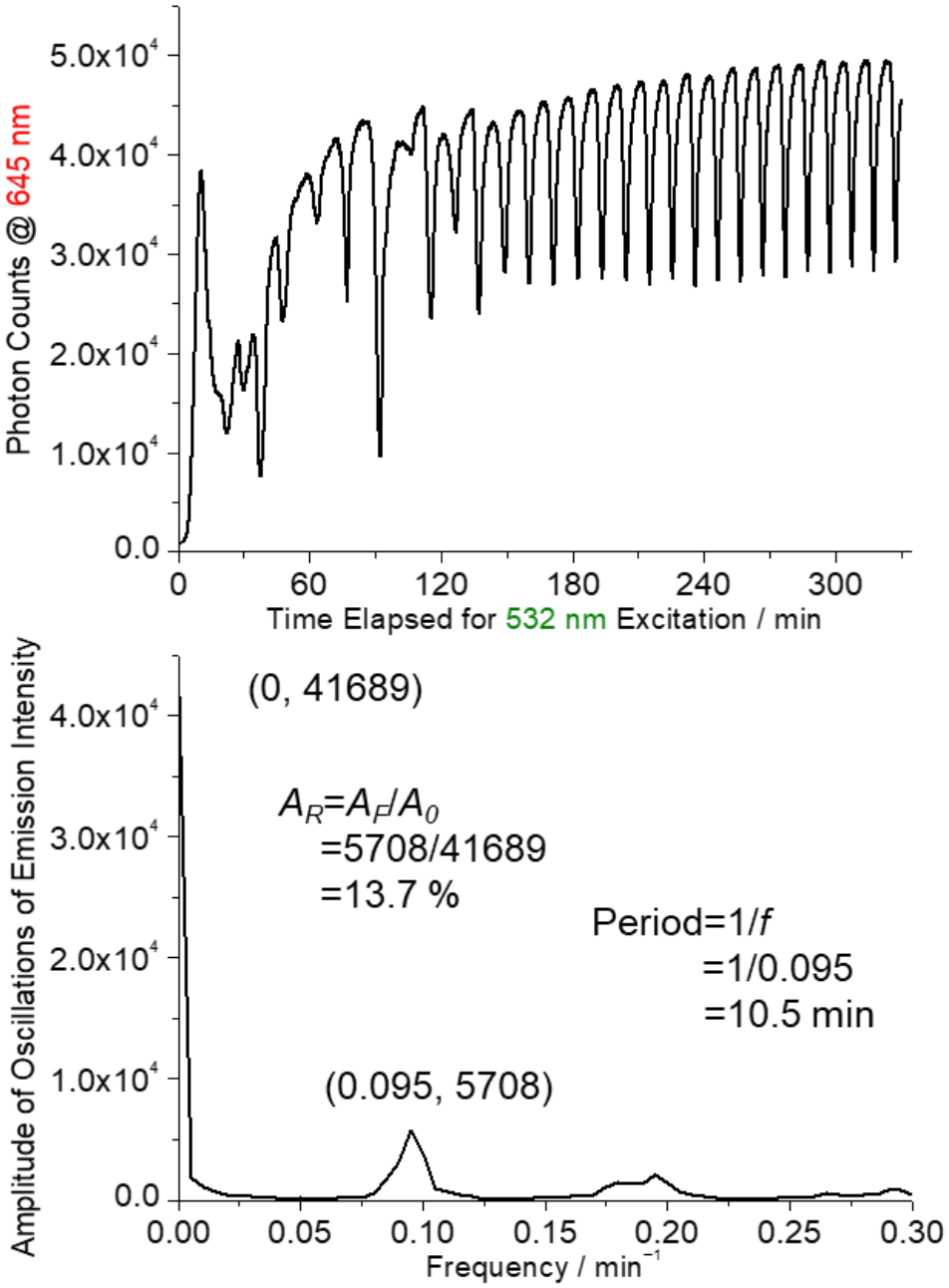

Figure S12. At another optical spectrum instrument, emission intensity of an aerated TMSO solution of Pt(OEP) (5.0×10^{-6} mol dm^{-3}) at 645 nm vs. time elapsed for 532 nm incoherent excitation of xenon lamp at 3.0 mW cm^{-2} when height is 6 mm at 25 °C, and its corresponding Fourier spectrum (calculated in the time window [125, 325] min).

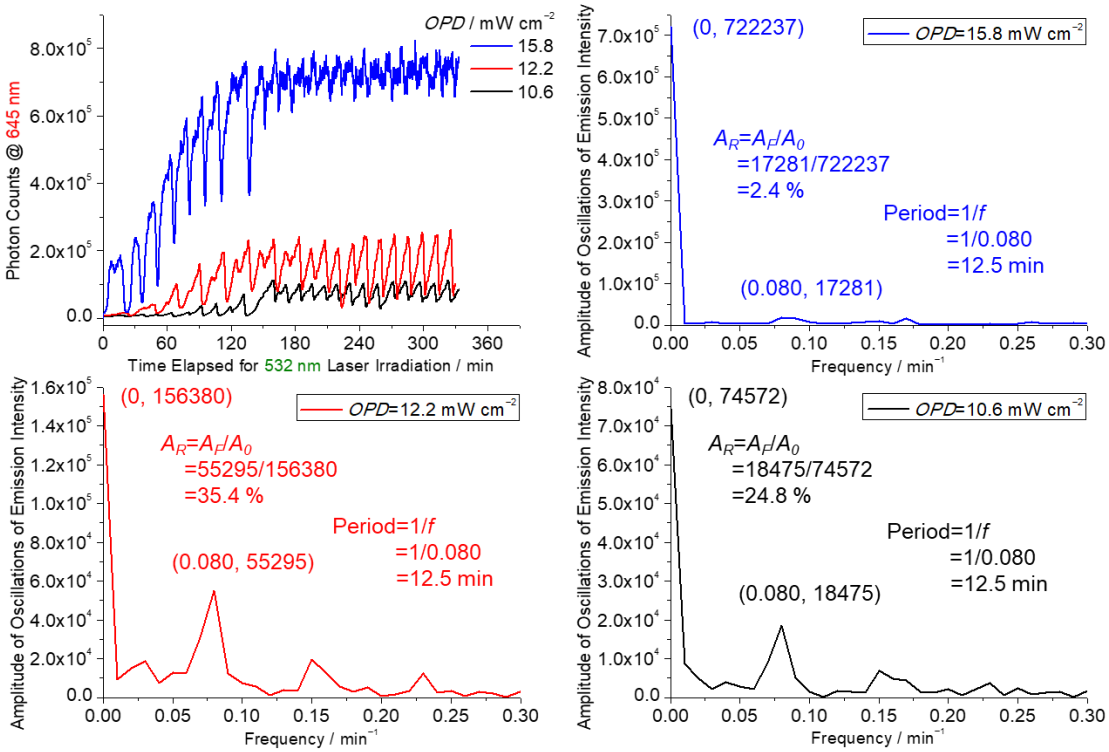

Figure S13. When height is 6 mm and concentration of Pt(OEP) is 5.0×10^{-6} mol dm^{-3}, emission intensity of an aerated TMSO solution upon coherent excitation of a 532 nm laser at different OPD, and their corresponding Fourier spectra (calculated in the time window [200, 300] min).

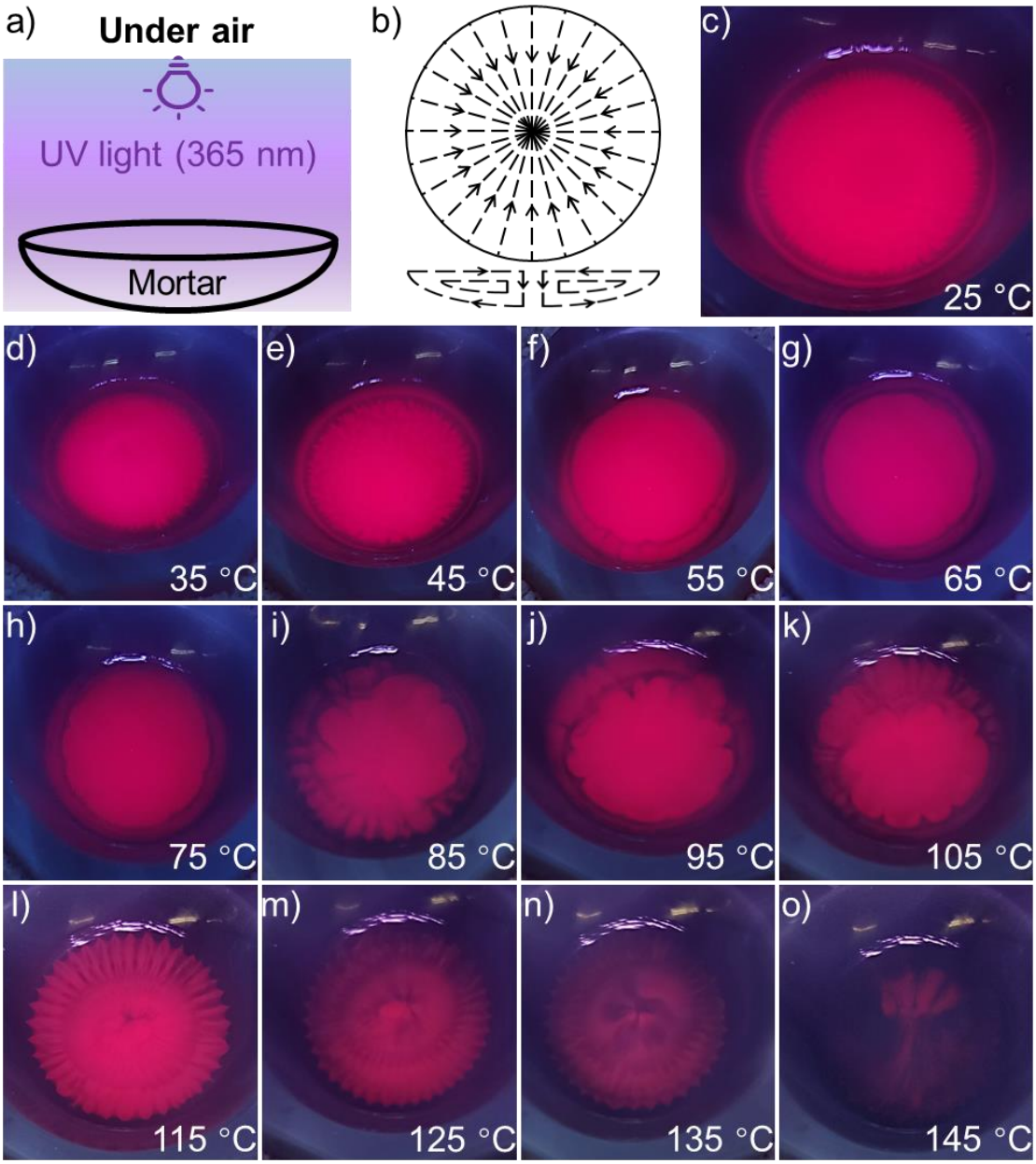

Figure S14. (a) Setup of the irradiation and heating system under air; (b) In a mortar, streamlines[3] of RB convection (RBC) on the upper interface (top) and a meridian plane (bottom); (c)-(o) Viewed from the top of mortar: Snapshots of an aerated TMSO solution of Pt(OEP) (5.0×10^{-6} mol dm^{-3}) upon 365 nm excitation of 33.3 mW cm^{-2} at different temperatures under air.

As shown in Fig. S14a, the irradiation and heating system was set up by heating the mortar bottom to control thermal gradient of RBC, whose streamlines were shown in Fig. S14b. The continuous excitation is homogeneous in space. As the photochemical deoxygenation proceeded under excitation, photo-activated phosphorescence (PAP) patterns that formed at a vary of temperatures were shown in Fig. S14c-o. When the mortar was left at 25 °C without heating, only a red uniform circle which was surrounded by tapered convexities, settled at the bottom of TMSO solution was

observed. When temperature was lower than 85 °C, observed patterns were uniform resulting from suppressed RBC whose driving force arising from buoyancy was too week to overcome the viscous resistance of solvent. A further increase in temperature triggered RBC, and then a symmetric loop of convection which in the central region descended to the mortar bottom and circled back to the mortar periphery, gradually occurred at ca. 115 °C. As a result, a red flower-like pattern, which was coincident with streamlines, generated. At 145 °C, patterns became asymmetric and disordered due to transition of RBC into asymmetric states of turbulent flow. In addition, all these patterns were settled at the mortar bottom, i.e., phosphorescence near the upper interface remained silent under air, implying sustainable transport of atmospheric oxygen into solution.

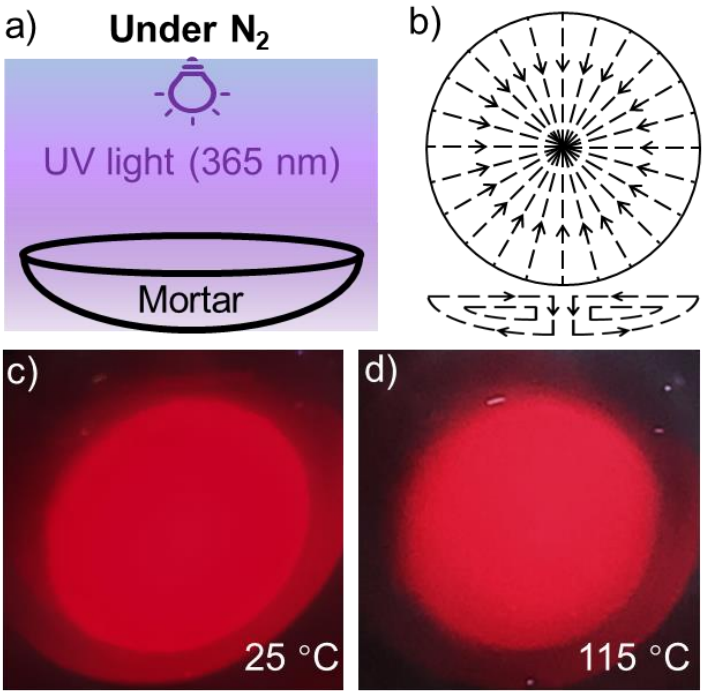

Figure S15. (a) The same setup of the irradiation and heating system under nitrogen; (b) In a mortar, streamlines[3] of RBC on the upper interface (top) and a meridian plane (bottom); (c) and (d) Viewed from the top of mortar: Snapshots of a N_2-bubbled TMSO solution of Pt(OEP) (5.0×10^{-6} mol dm^{-3}) upon UV irradiation of 33.3 mW cm^{-2} at different temperatures under N_2.

Replacing oxygen with nitrogen, only a uniform circle spread throughout solution was observed, no matter how to heat.

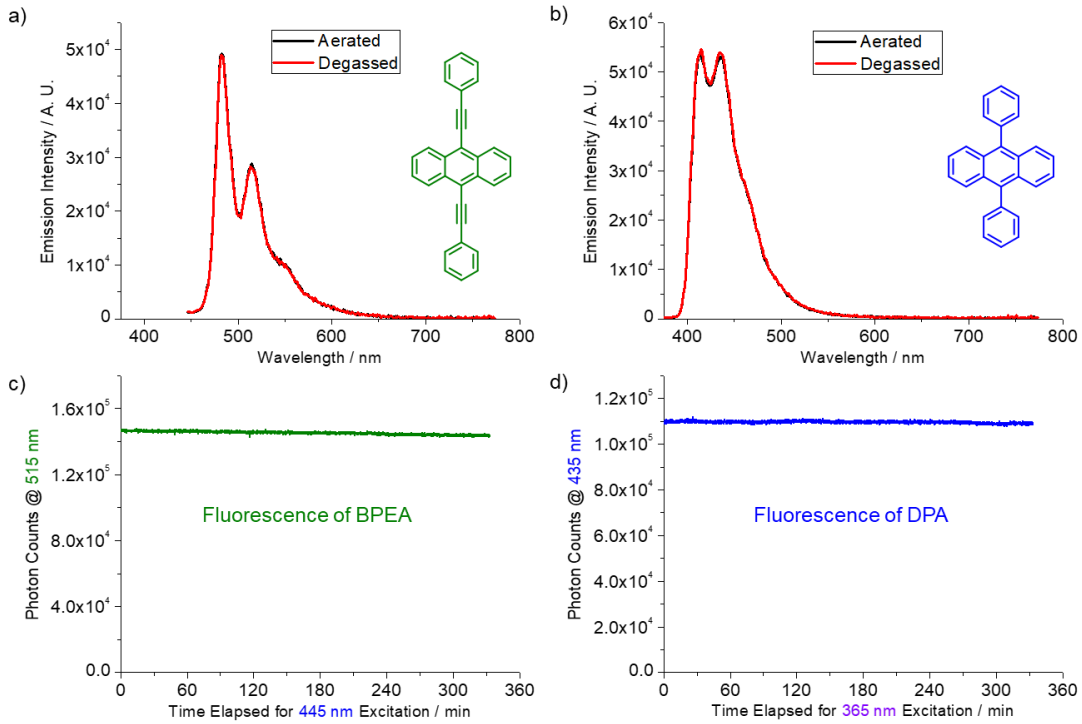

Figure S16. (a) Emission spectrum of BPEA (5.0×10^{-6} mol dm^{-3}) in an aerated (black line)/degassed (red line) TMSO solution upon 445 nm excitation of xenon lamp; (b) Emission spectrum of DPA (5.0×10^{-6} mol dm^{-3}) in an aerated (black line)/degassed (red line) TMSO solution upon 365 nm excitation of xenon lamp; (c)/(d) Emission intensity of aerated TMSO solution of BPEA/DPA (5.0×10^{-6} mol dm^{-3}) at 515/435 nm vs. time elapsed for 445/365 nm incoherent excitation of xenon lamp at 1.1 mW cm^{-2} under air.

It was widely accepted that fluorophores were generally not efficient photo-sensitizers which could sensitize molecular oxygen into singlet oxygen, that is, molecular oxygen couldn't usually quench emission of singlet excited states of fluorophores. Replacing phosphors with fluorophores (such as BPEA or DPA) as the solute whose emission was (green or bule) fluorescence, the emission intensity kept steady over excitation time under air, also implying that the OPD of excitation of xenon lamp was constant.

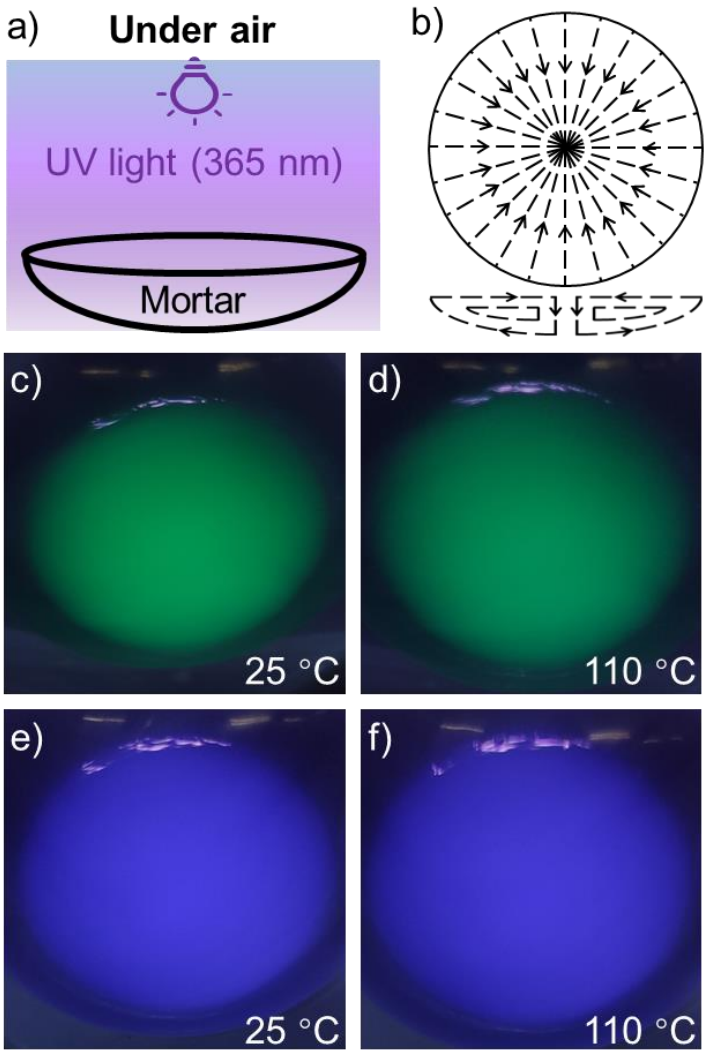

Figure S17. (a) The same setup of the irradiation and heating system under air; (b) In a mortar, streamlines[3] of RBC on the upper interface (top) and a meridian plane (bottom); Viewed from the top of mortar: (c) and (d) Snapshots of an aerated TMSO solution of BPEA (5.0×10^{-6} mol dm^{-3}) upon 365 nm excitation of 33.3 mW cm^{-2} at different temperatures under air; (e) and (f) Snapshots of an aerated TMSO solution of DPA (5.0×10^{-6} mol dm^{-3}) upon 365 nm excitation of 33.3 mW cm^{-2} at different temperatures under air.

Replacing Pt(OEP) with fluorophores (such as BPEA or DPA) as the solute, here was a uniform circle spread throughout solution, no matter how to heat.

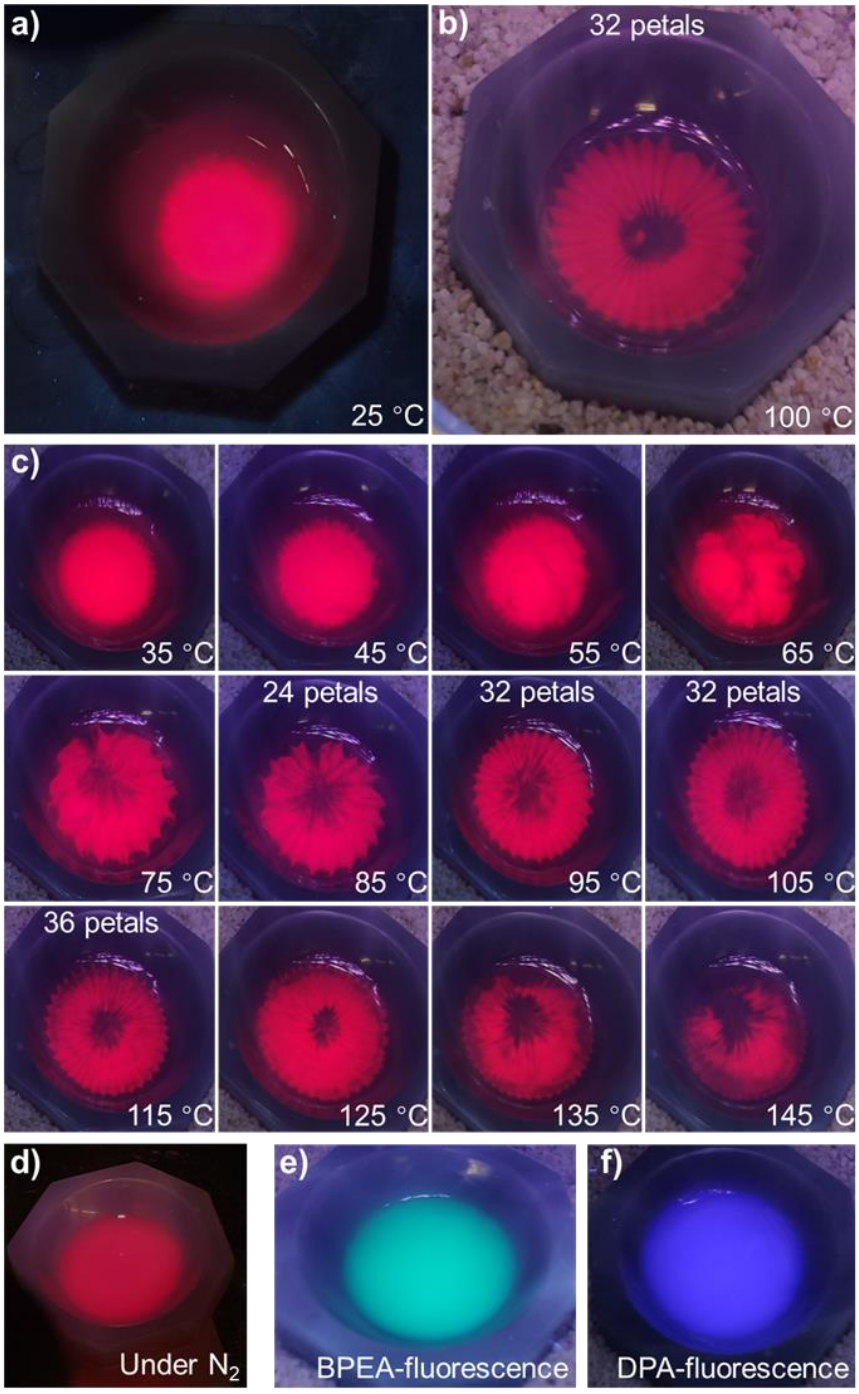

Figure S18. The same experimental condition as the TMSO solution. Viewed from the top of mortar: (a-c) Snapshots of an aerated DMSO solution of Pt(OEP) (5.0×10^{-6} mol dm^{-3}) upon 365 nm excitation of 33.3 mW cm^{-2}; (d) A snapshot of a N_2-bubbled DMSO solution of Pt(OEP) (5.0×10^{-6} mol dm^{-3}) under N_2 upon 365 nm excitation of 33.3 mW cm^{-2}; (e)/(f) A snapshot of an aerated DMSO solution of BPEA/DPA (5.0×10^{-6} mol dm^{-3}) upon 365 nm excitation of 33.3 mW cm^{-2}. No matter how to heat, only a uniform circle spread throughout solution was observed in (d), (e) and (f).

All these photochemical reaction-diffusion-convection phenomena of flower-like patterns were reproduced well in DMSO.

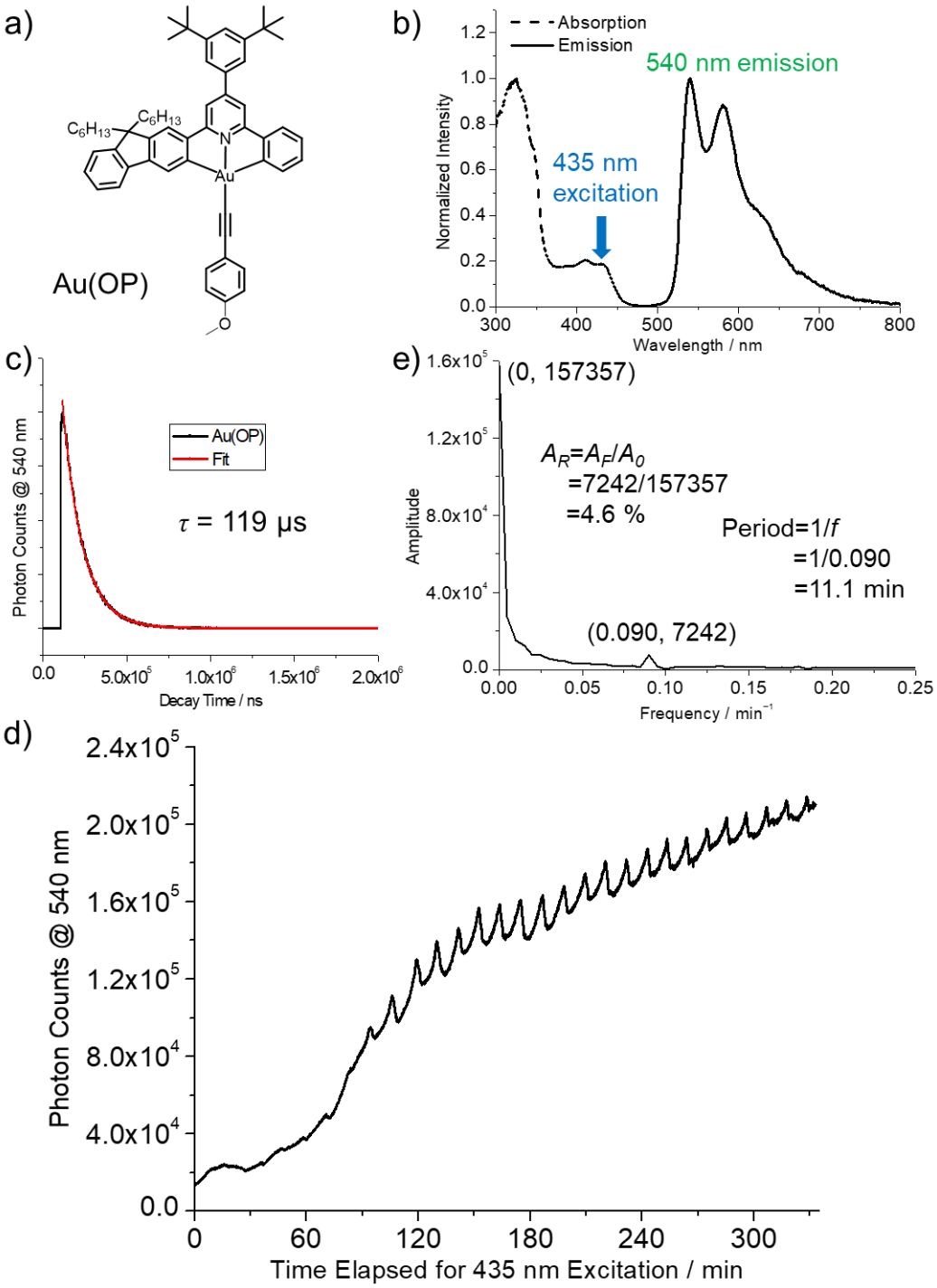

Figure S19. (a) The chemical structure of Au(OP); (b) Absorption and emission spectra of Au(OP) in a N_2-bubbled TMSO solution; (c) Lifetime of a N_2-bubbled TMSO solution of Au(OP) (50.0×10^{-6} mol dm^{-3}) upon excitation at 435 nm, and its quantum yield is 24 %; (d) Emission intensity of an aerated TMSO solution of Au(OP) (50.0×10^{-6} mol dm^{-3}) at 540 nm vs. time elapsed for 435 nm incoherent excitation of xenon lamp at 0.5 mW cm^{-2}; (e) The corresponding Fourier spectrum (calculated in the time window [100, 300] min) of emission spectrum.

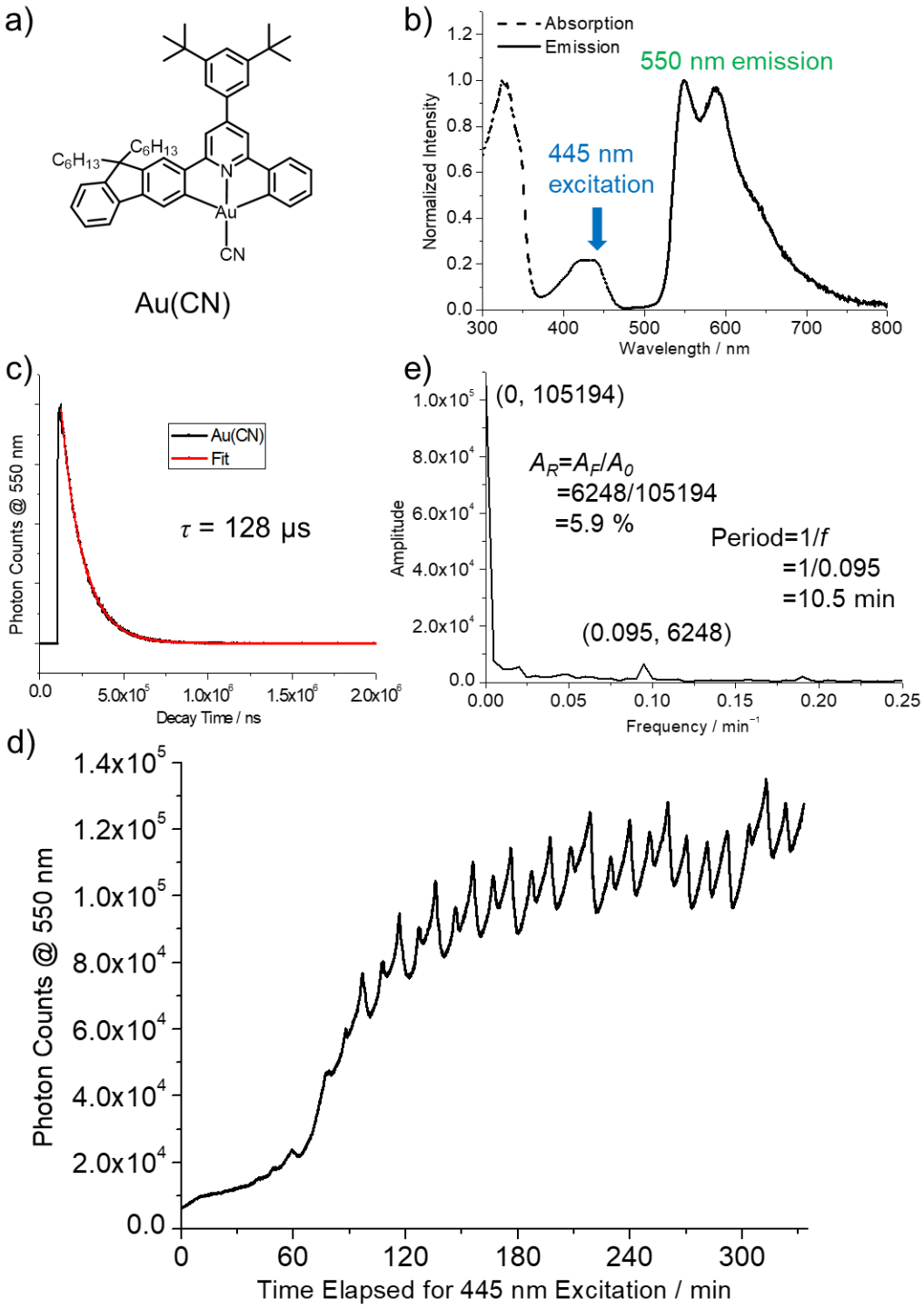

Figure S20. (a) The chemical structure of Au(CN); (b) Absorption and emission spectra of Au(CN) in a N_2-bubbled TMSO solution; (c) Lifetime of a N_2-bubbled TMSO solution of Au(CN) (50.0×10^{-6} mol dm^{-3}) upon excitation at 445 nm, and its quantum yield is 16 %; (d) Emission intensity of an aerated TMSO solution of Au(CN) (50.0×10^{-6} mol dm^{-3}) at 550 nm vs. time elapsed for 445 nm incoherent excitation of xenon lamp at 0.6 mW cm^{-2}; (e) The corresponding Fourier spectrum (calculated in the time window [125, 325] min) of emission spectrum.

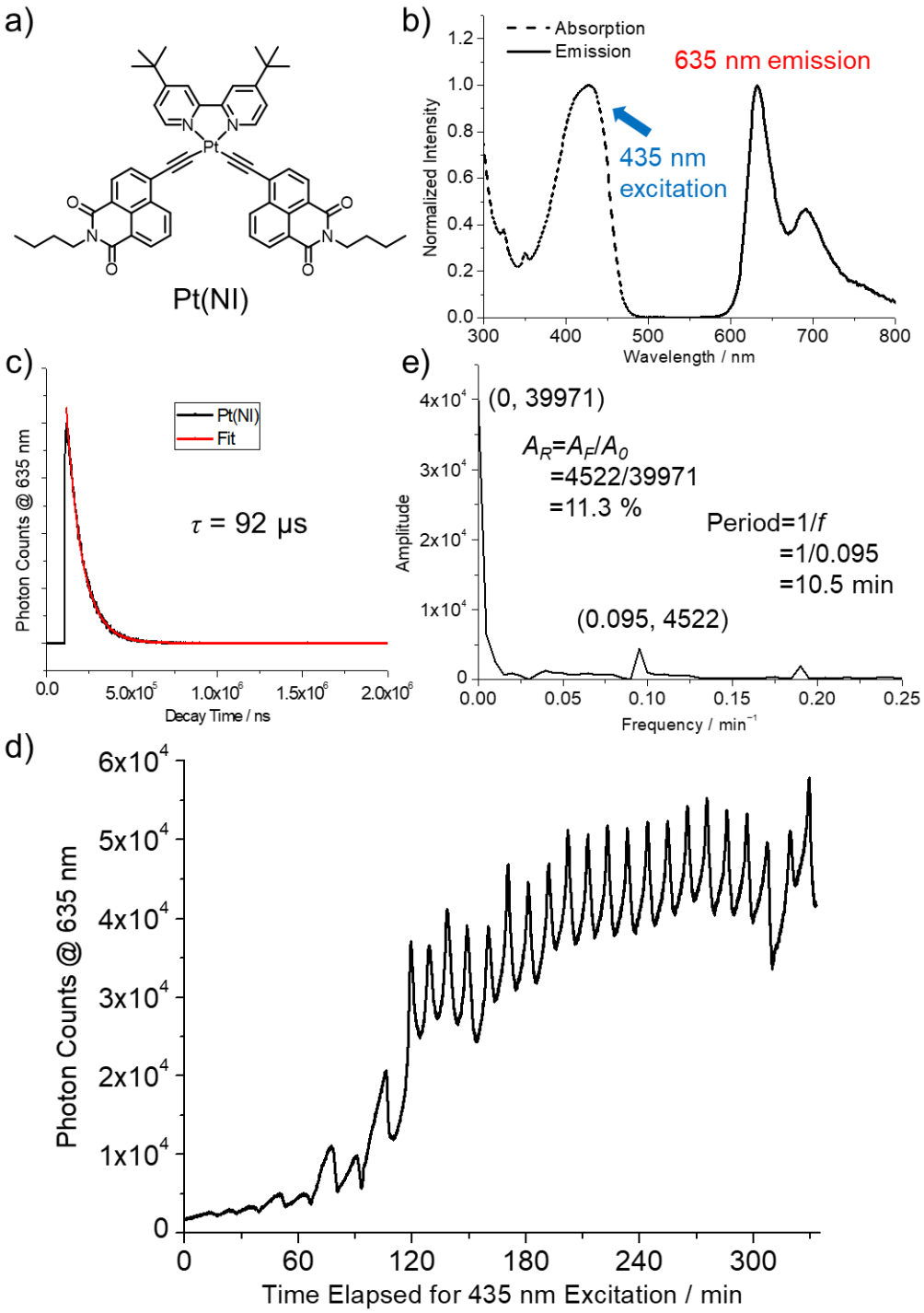

Figure S21. (a) The chemical structure of Pt(NI); (b) Absorption and emission spectra of Pt(NI) in a N_2-bubbled TMSO solution; (c) Lifetime of a N_2-bubbled TMSO solution of Pt(NI) (20.0×10^{-6} mol dm^{-3}) upon excitation at 435 nm, and its quantum yield is 15 %; (d) Emission intensity of an aerated TMSO solution of Pt(NI) (30.0×10^{-6} mol dm^{-3}) at 635 nm vs. time elapsed for 435 nm incoherent excitation of xenon lamp at 0.5 mW cm^{-2}; (e) The corresponding Fourier spectrum (calculated in the time window [125, 325] min) of emission spectrum.

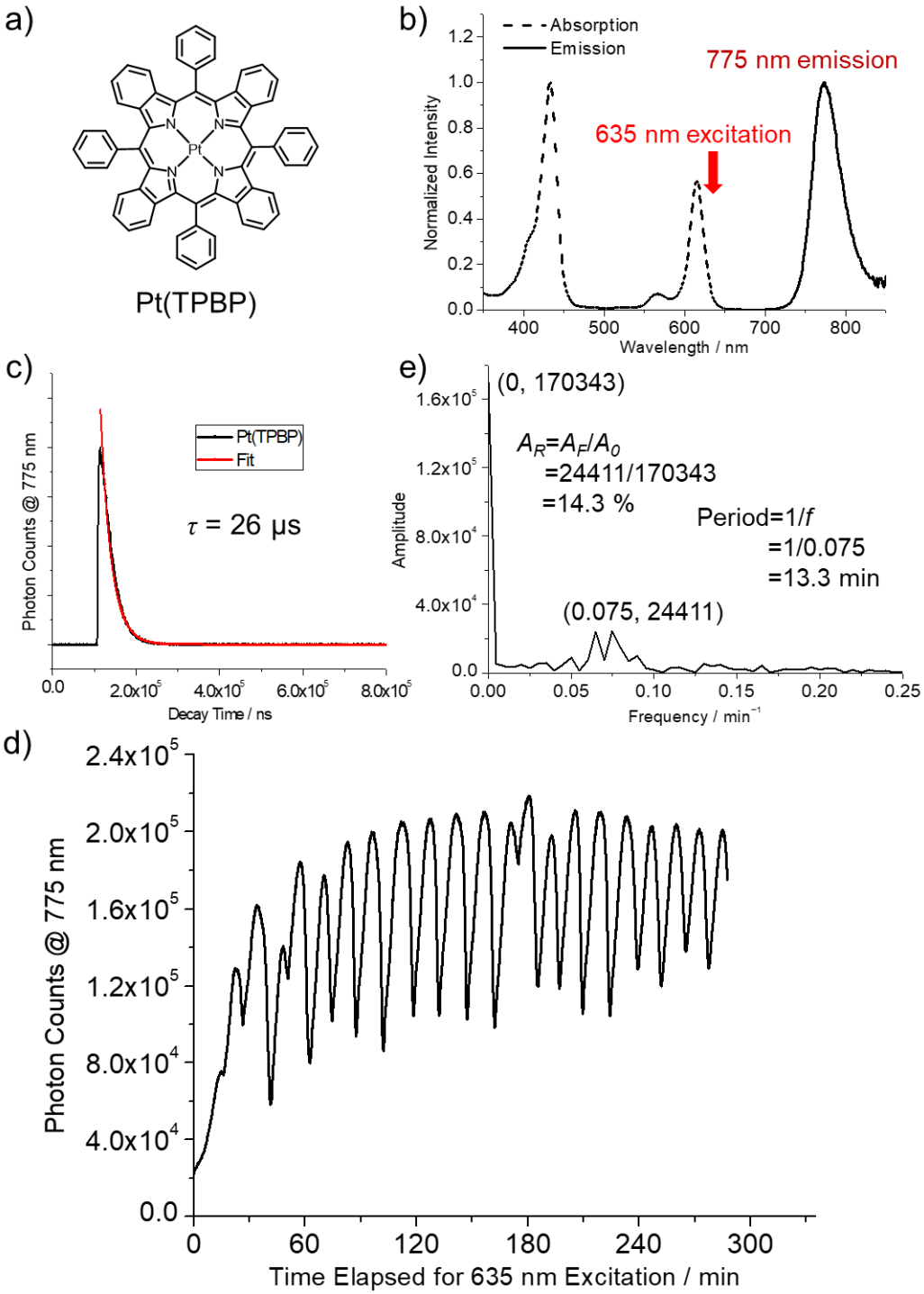

Figure S22. (a) The chemical structure of Pt(TPBP); (b) Absorption and emission spectra of Pt(TPBP) in a N_2-bubbled TMSO solution; (c) Lifetime of a N_2-bubbled TMSO solution of Pt(TPBP) (10.0×10^{-6} mol dm^{-3}) upon excitation at 635 nm, and its quantum yield is 15 %; (d) Emission intensity of an aerated TMSO solution of Pt(TPBP) (10.0×10^{-6} mol dm^{-3}) at 775 nm vs. time elapsed for 635 nm incoherent excitation of xenon lamp at 2.1 mW cm^{-2}; (e) The corresponding Fourier spectrum (calculated in the time window [75, 275] min) of emission spectrum.

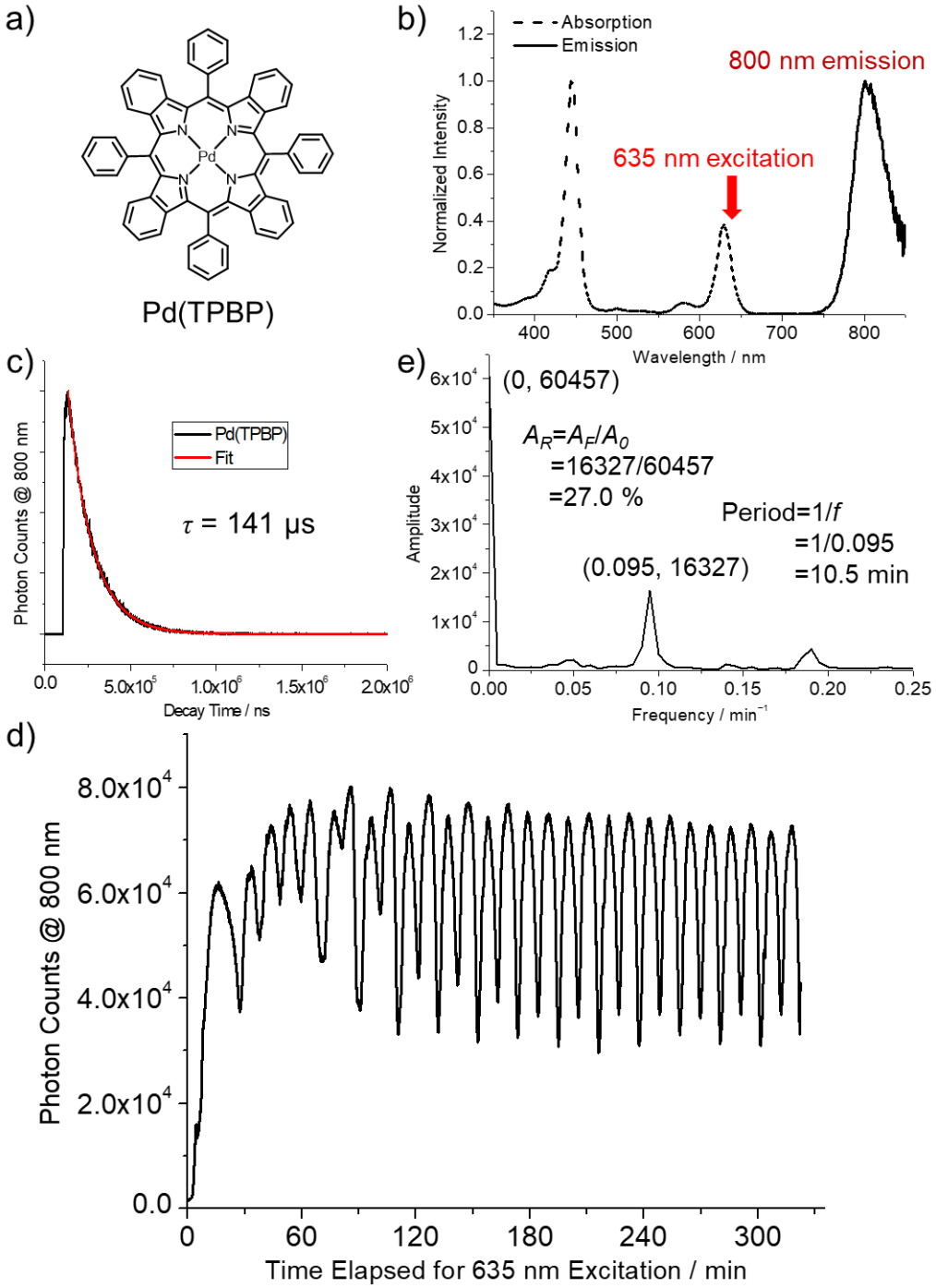

Figure S23. (a) The chemical structure of Pd(TPBP); (b) Absorption and emission spectra of Pd(TPBP) in a N_2-bubbled TMSO solution; (c) Lifetime of a N_2-bubbled TMSO solution of Pd(TPBP) (10.0×10^{-6} mol dm^{-3}) upon excitation at 635 nm, and its quantum yield is 6 %; (d) Emission intensity of an aerated TMSO solution of Pd(TPBP) (5.0×10^{-6} mol dm^{-3}) at 800 nm vs. time elapsed for 635 nm incoherent excitation of xenon lamp at 2.1 mW cm^{-2}; (e) The corresponding Fourier spectrum (calculated in the time window [120, 320] min) of emission spectrum.

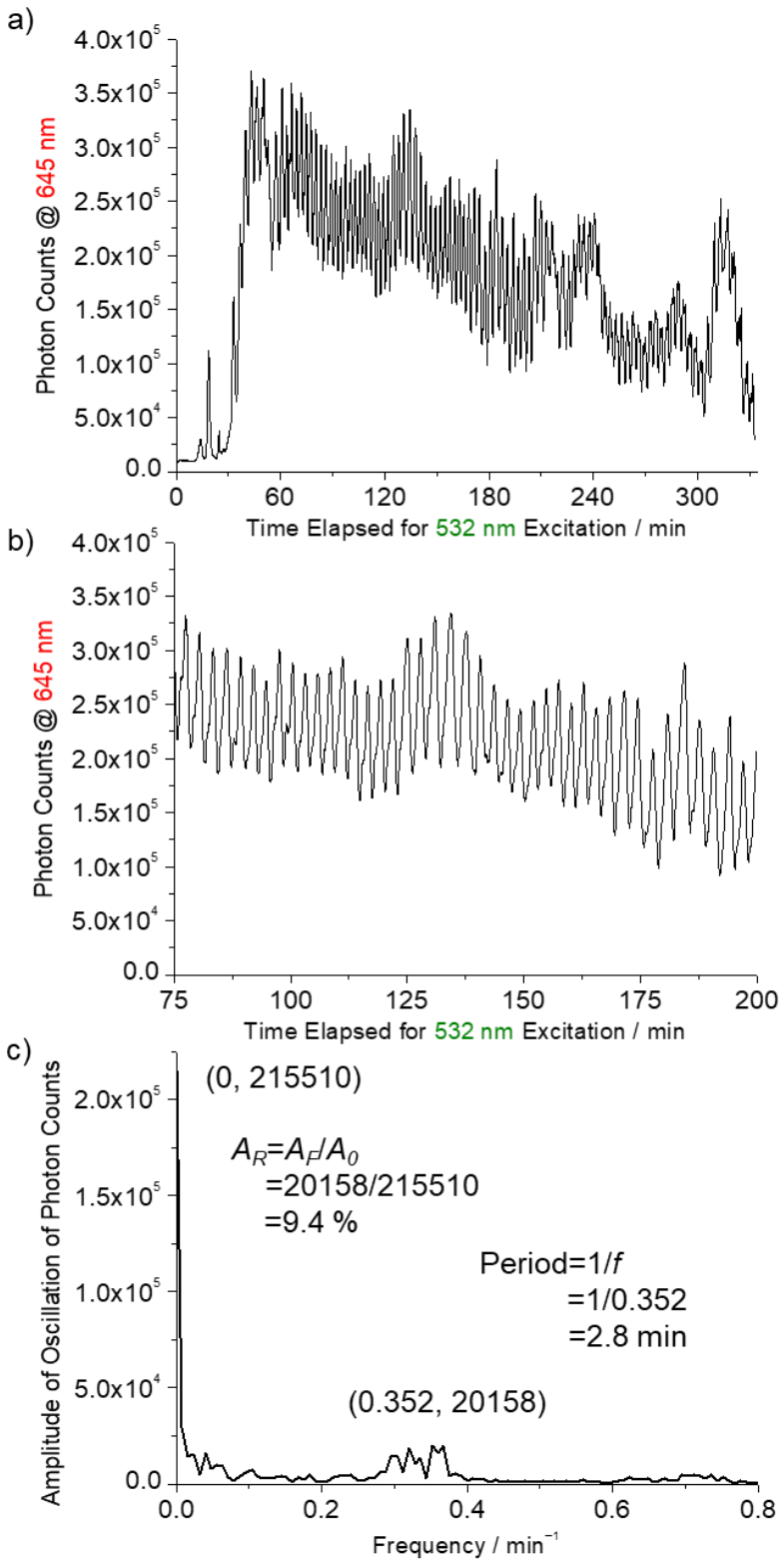

Figure S24. (a) Emission intensity of an aerated DMSO solution of Pt(OEP) (10.0×10^{-6} mol dm^{-3}) at 645 nm vs. time elapsed for 532 nm incoherent excitation of xenon lamp at 1.1 mW cm^{-2} when height is 3 mm at 25 °C; (b) Enlargement of the emission spectrum showing uneven oscillations, whose Fourier spectrum (calculated in the time window [75, 200] min) is depicted in (c).

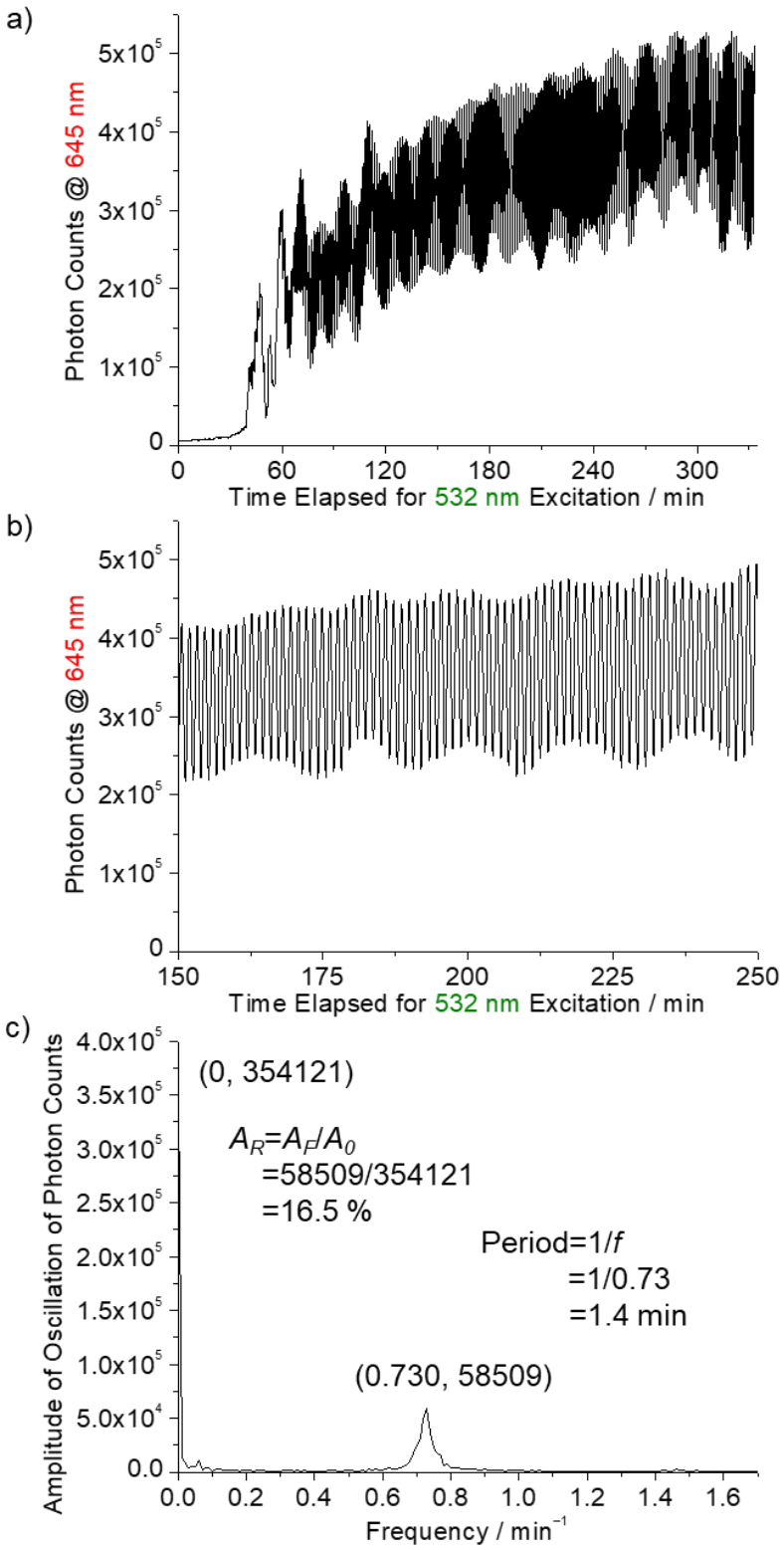

Figure S25. (a) Emission intensity of an aerated DMPU solution of Pt(OEP) (10.0×10^{-6} mol dm^{-3}) at 645 nm vs. time elapsed for 532 nm incoherent excitation of xenon lamp at 16.0 mW cm^{-2} when height is 21 mm at 25 °C; (b) Enlargement of the emission spectrum showing regular oscillations, whose Fourier spectrum (calculated in the time window [150, 250] min) is depicted in (c).

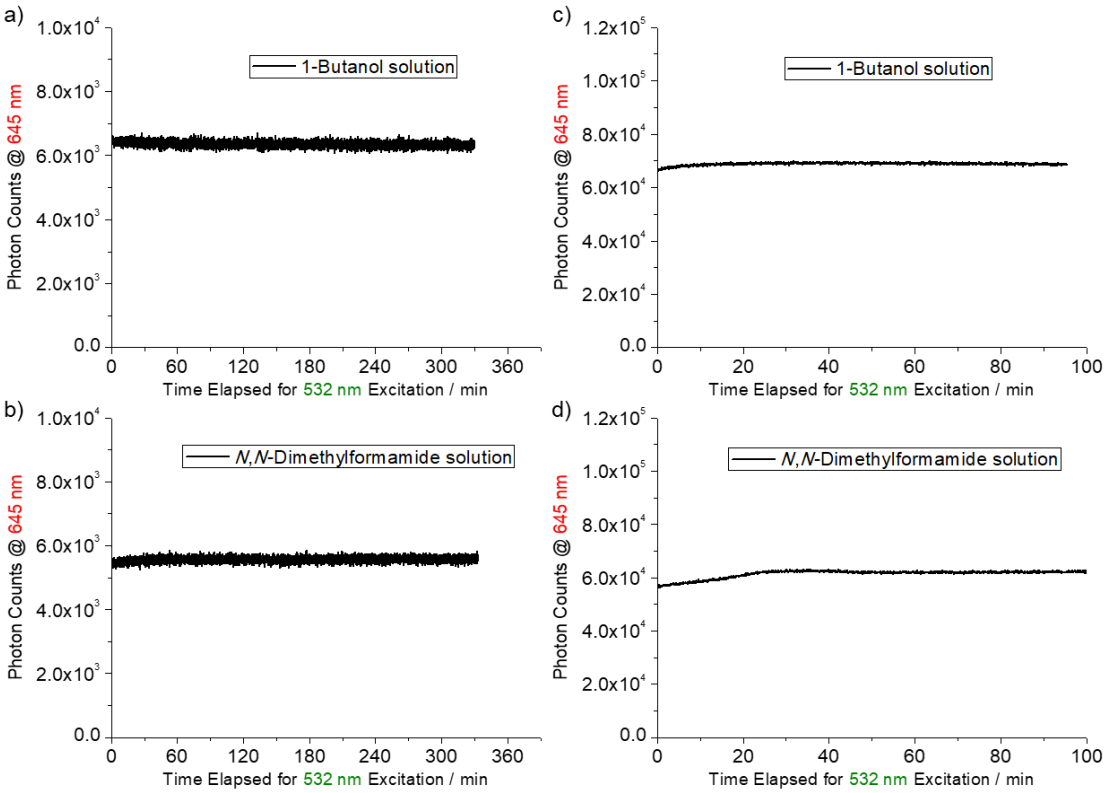

Figure S26. Emission intensity of an aerated 1-butanol/*N*, *N*-dimethylformamide solution of Pt(OEP) (5.0×10^{-6} mol dm^{-3}) at 645 nm vs. time elapsed for 532 nm incoherent excitation of xenon lamp at 1.1 (a-b)/13.5 (c-d) mW cm^{-2} when height is 6 mm at 25 ºC.

In contrast, TMSO was replaced with 1-butanol and *N*, *N*-dimethyl-formamide which were inert solvents for scavenging singlet oxygen. In these inert solvents, no oscillation was found because emission of Pt(OEP) kept silent and constant at the incipient intensity while the solution was always saturated with molecular oxygen.

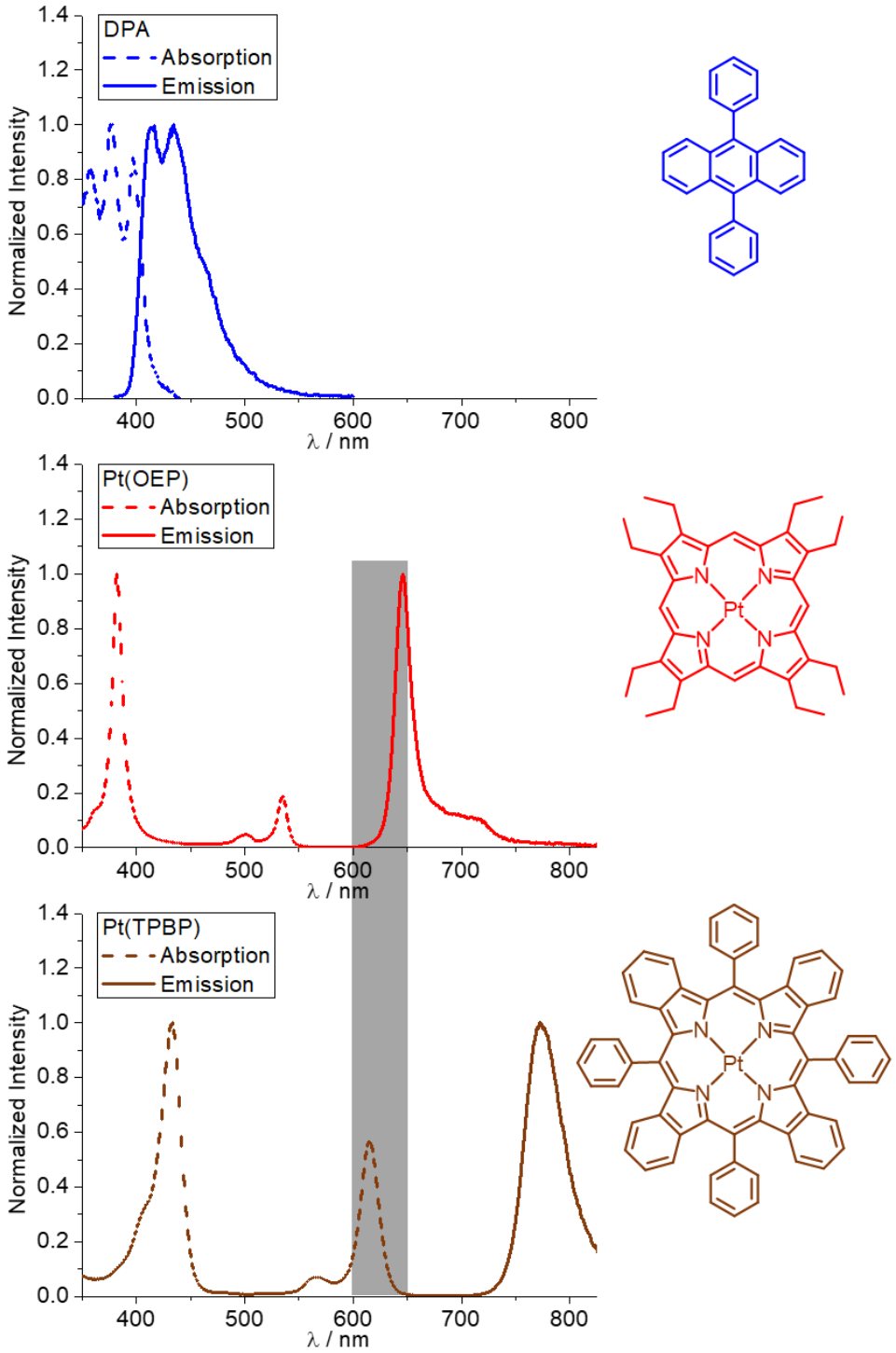

Figure S27. Absorption and emission spectra of DPA, Pt(OEP) and Pt(TPBP) in TMSO.

There was an overlap (600–650 nm) between the emission spectrum of Pt(OEP) and the absorption spectrum of Pt(TPBP).

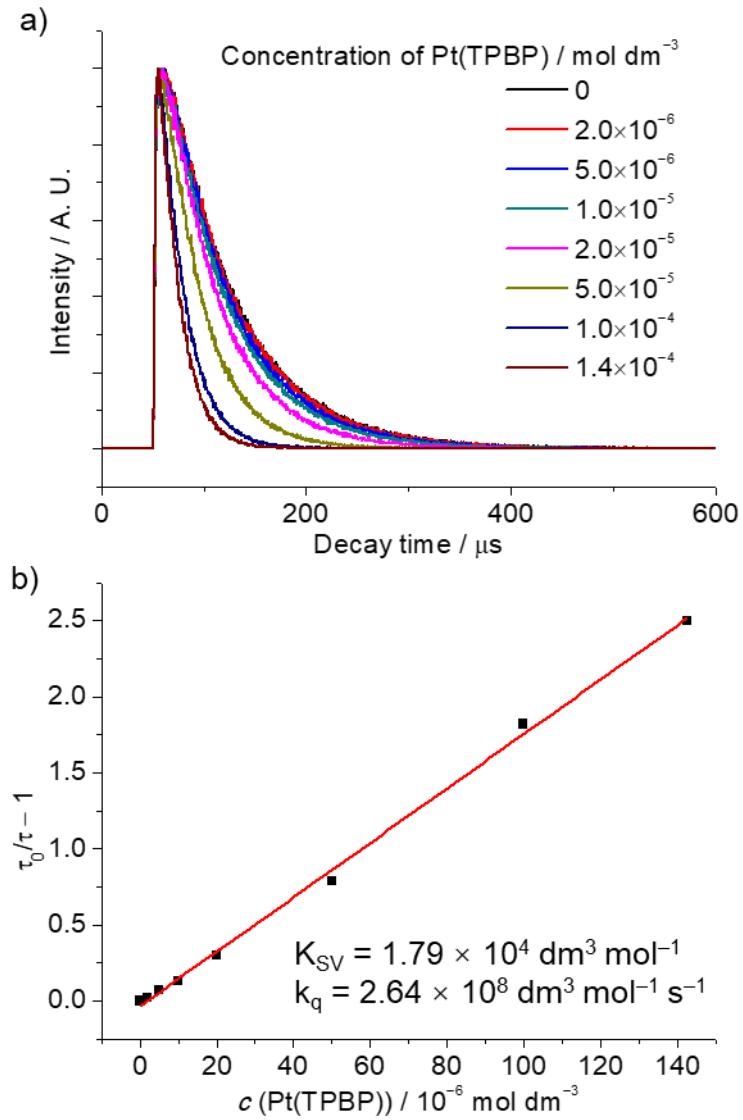

Figure S28. Decay curves of the 645 nm phosphorescence of Pt(OEP) in the presence of different concentration of Pt(TPBP) in aerated TMSO solutions after photo-activation. (b) Stern−Volmer analysis of dynamic quenching between Pt(OEP) and Pt(TPBP) in TMSO solutions under air.

For triplet-to-triplet energy transfer (TTET) down-conversion of Pt(OEP) and Pt(TPBP), the bimolecular quenching rate constant (k_q) was 2.64 × 10^8 dm^3 mol^{-1} s^{-1}.

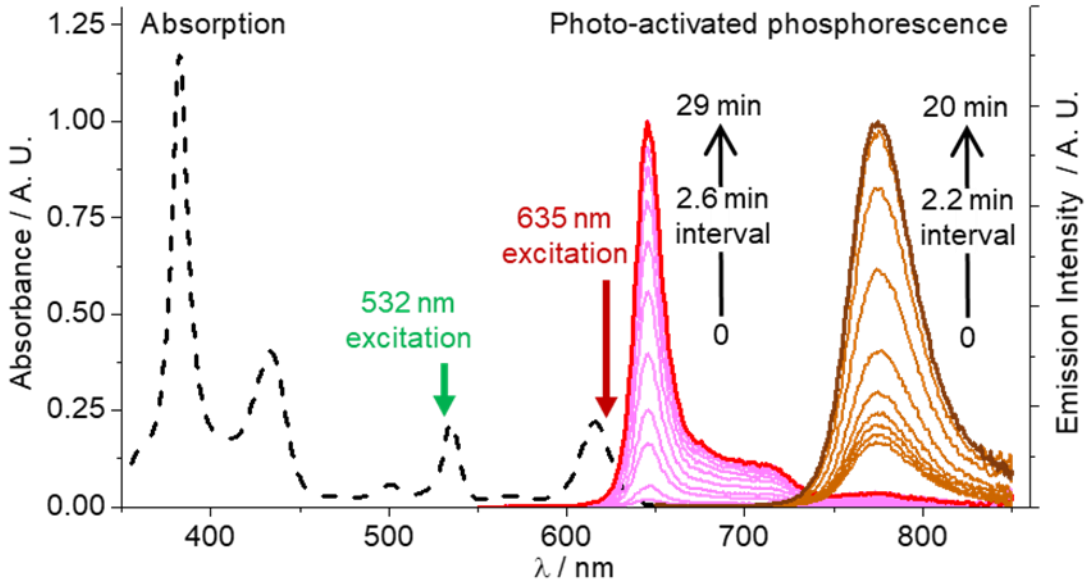

Figure S29. An aerated TMSO solution of Pt(OEP) (5.0×10^{-6} mol dm^{-3}) and Pt(TPBP) (2.0×10^{-6} mol dm^{-3}) under air: Absorption spectrum, and emission spectra upon 532 nm (7.1 mW cm^{-2}) or 635 nm (6.4 mW cm^{-2}) continuous excitation by a xenon lamp when *h* is 15 mm.

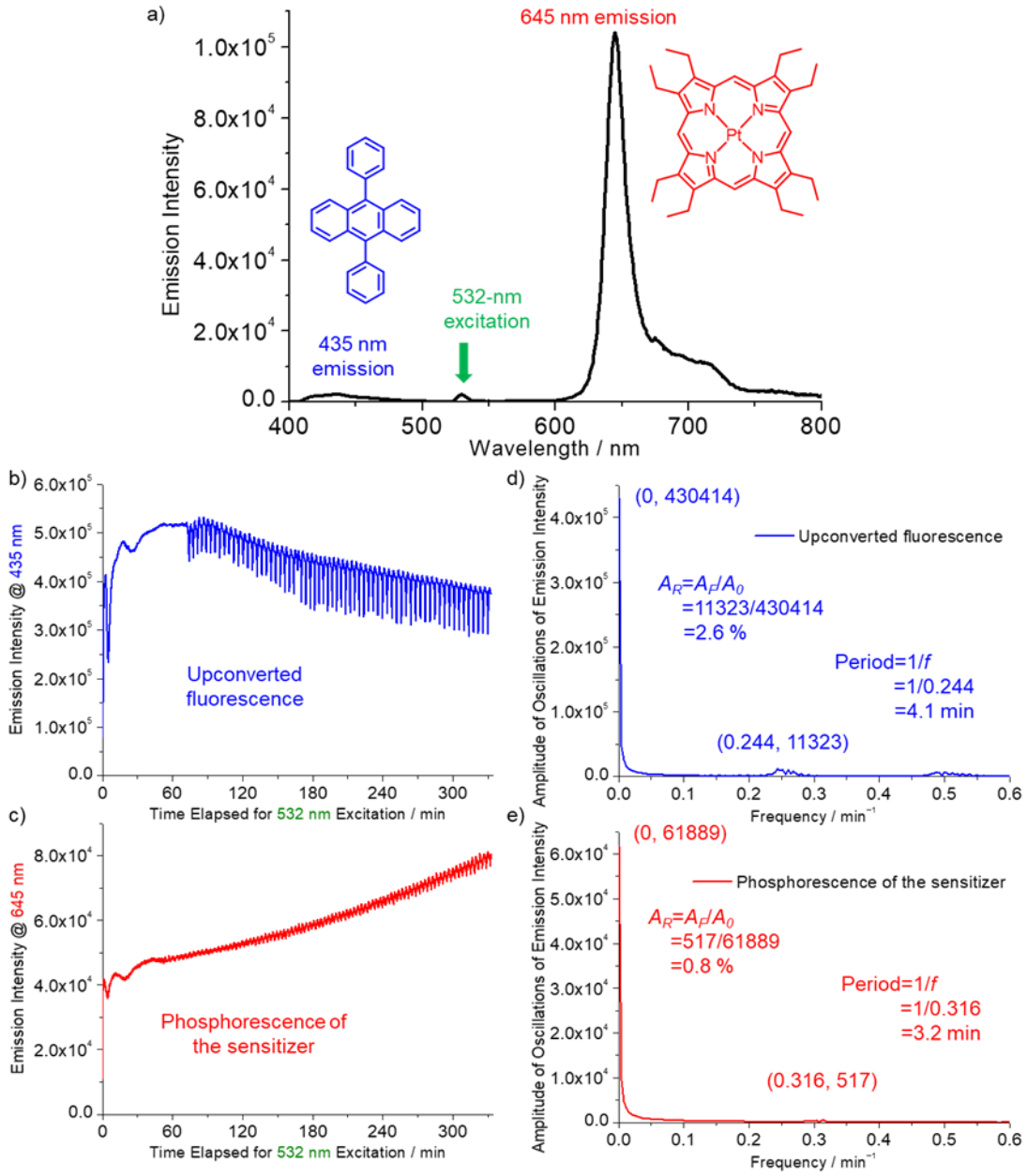

Figure S30. In an aerated TMSO solution of Pt(OEP) (10.0×10^{-6} mol dm^{-3}) and DPA (1.0×10^{-3} mol dm^{-3}) upon 532 nm incoherent excitation of xenon lamp at 13.7 mW cm^{-2} at 21 °C under air when height is 3 mm: (a) the emission spectrum after being photoactivated; (b)/(c) emission intensity at 435/645 nm vs. irradiation time; (d) and (e) the corresponding Fourier spectra (calculated in the time window [75, 325] min) of (b) and (c), respectively.

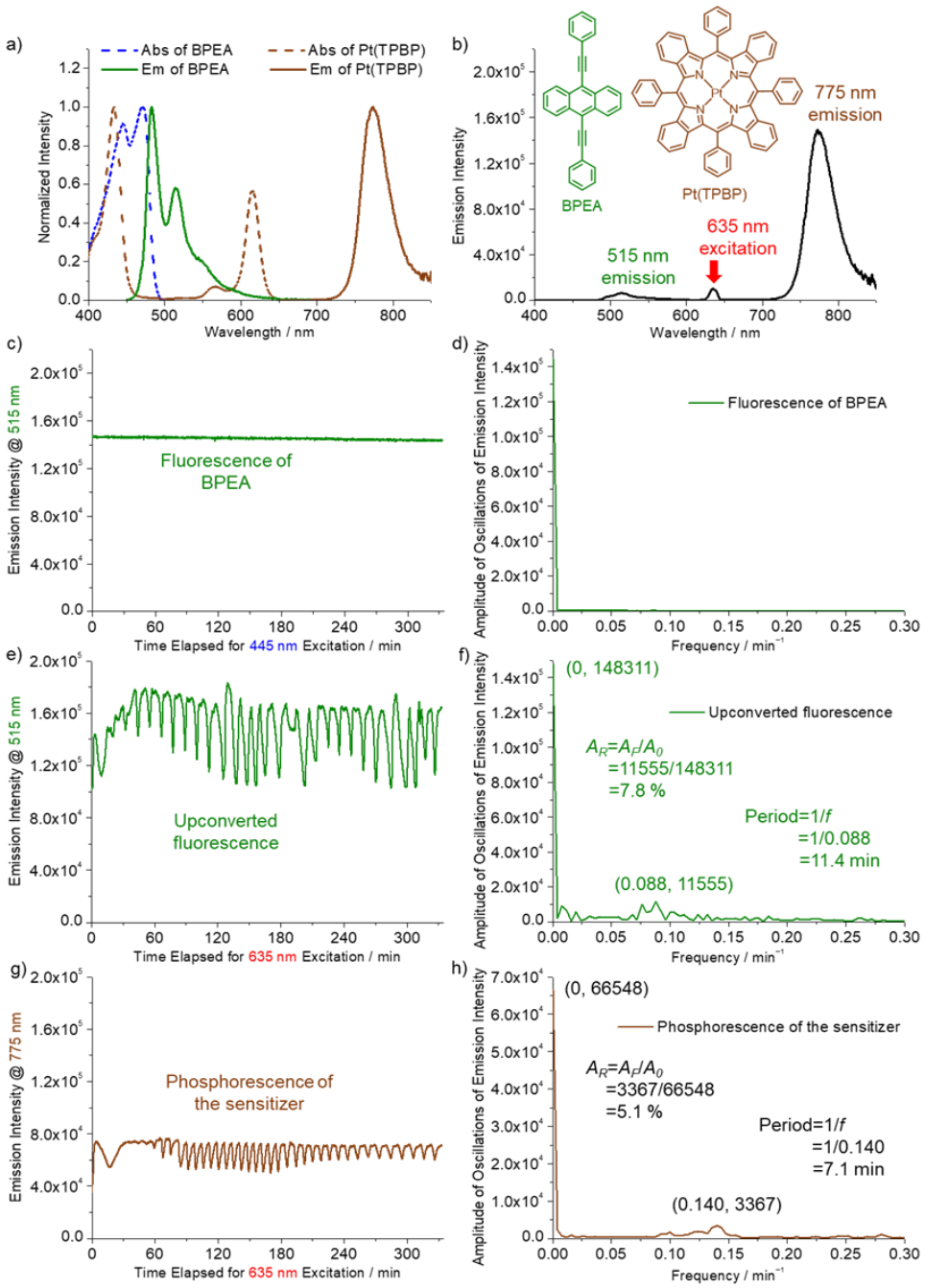

Figure S31. (a) The absorption and emission spectra of Pt(TPBP)/BPEA in TMSO solutions; (c) Emission intensity of TMSO solution of BPEA (5.0×10^{-6} mol dm^{-3}) at 515 nm vs. time elapsed for 445 nm incoherent excitation of xenon lamp at 21 °C under air, and (d) the corresponding Fourier spectra (calculated in the time window [75, 325] min) of (c); (b) and (e)-(h) In an aerated TMSO solution of Pt(TPBP) (10.0×10^{-6} mol dm^{-3}) and BPEA (1.0×10^{-3} mol dm^{-3}) upon 635 nm incoherent excitation of xenon lamp at 5.5 mW cm^{-2} at 21 °C under air when height is 3 mm: (b) the emission spectrum after being photoactivated; (e)/(g) emission intensity at 515/775 nm vs. irradiation time, and (f)/(h) the corresponding Fourier spectra (calculated in the time window [75, 325] min) of (e)/(g).

References

(S1) H. M. Guo, M. L. Muro-Small, S. M. Ji, J. Z. Zhao and F. N. Castellano, *Inorg. Chem.*, 2010, **49**, 6802.

(S2) W. P. To, K. T. Chan, G. S. M. Tong, C. S. Ma, W. M. Kwok, X. G. Guan, K. H. Low and C. M. Che, *Angew. Chem. Int. Ed.*, 2013, **52**, 6648.

(S3) Y. H. Chen, Y. F. Liu, S. Lu, S. Ye, H. Gu, J. Qiang, Y. R. Li and X. Q. Chen, *J. Am. Chem. Soc.*, 2020, **142**, 20066.